Journal of Computational Physics 229 (2010) 4501–4521

Contents lists available at ScienceDirect

Journal of Computational Physics

journal homepage: www.elsevier.com/locate/jcp

An efficient S-DDM iterative approach for compressible contamination fluid flows in porous media

Chuanbin Du, Dong Liang *

Department of Mathematics and Statistics, York University, Toronto, Ontario, Canada M3J 1P3

ARTICLE INFO

Article history:
Received 18 January 2009
Received in revised form 7 February 2010
Accepted 17 February 2010
Available online 6 March 2010

Keywords:
Compressible contamination flow
Porous media
Domain decomposition
Non-overlapping
Splitting
Extrapolation

ABSTRACT

In this paper, we develop an efficient splitting domain decomposition method (S-DDM) for compressible contamination fluid flows in porous media over multiple block-divided sub-domains by combining the non-overlapping domain decomposition, splitting, linearization and extrapolation techniques. The proposed S-DDM iterative approach divides the large domain into multiple block sub-domains. In each time interval, the S-DDM scheme is applied to solve the water head equation, in which an efficient local multilevel scheme is used for computing the values of water head on the interfaces of sub-domains, and the splitting implicit scheme is used for computing the interior values of water head in sub-domains; and the S-DDM scheme is then proposed to solve the concentration equation by combining the upstream volume technique. Numerical experiments are performed and analyzed to illustrate the efficiency of the S-DDM iterative approach for simulating compressible contamination fluid flows in porous media. The developed method takes the excellent attractive advantages of both the non-overlapping domain decomposition and the splitting technique, and reduces computational complexities, large memory requirements and long computational durations.

1. Introduction

Compressible fluid flows in porous media have widely been encountered in many areas of computational simulations in science and engineering, e.g. groundwater contamination, seawater intrusion in coastal aquifers, environment protection, hazardous waste deposition, and oil recovery in reservoir (see [1,3,6,10,14,26]). The objective of simulating fluid flows in porous media is to quantify the transport of the pollutants, to predict, control, and re-mediate contaminations in subsurface contaminant transports and re-mediations, seawater intrusion and control, and many other applications. The mathematical model of contamination fluid flows in porous media is a coupled nonlinear system of time-dependent partial differential equations, in which one equation is a parabolic equation and the other is a convection–diffusion equation. The model is characterized by the nonlinearity, the coupling of these equations, the advection dominance of the transport equation, the moving steep fronts present in the solutions, the compressibility of the fluid mixture and the medium, the heterogeneity of media, the enormous size of field-scale applications, and the required long time period of prediction. From a practical point of view, numerical methods play a major role in modeling of fluid flows in porous media. As we know, the interests in numerical computations of fluid flows in porous media have been rising rapidly and numerical simulations have been more and more indispensable (see [2,6,15,16,27]). Due to the computational complexities and the huge computational costs in realistic long term and large scale applications, there are strong interests in developing efficient solution techniques for large scale applications of compressible fluid flows in porous media.

* Corresponding author. Tel.: +1 416 736 2100; fax: +1 416 736 5757.
E-mail address: dliang@mathstat.yorku.ca (D. Liang).

0021-9991/$ - see front matter © 2010 Elsevier Inc. All rights reserved.
doi:10.1016/j.jcp.2010.02.019

Domain decomposition methods allow the reduction of the sizes of problems by decomposing domain into smaller ones on which the problems can be solved by multiple computers in parallel (see [9,13,18,23,24,29], etc). The splitting technique is another attractive and popular technique to reduce high-dimensional problems to a series of one-dimensional problems at each time step for saving the memory and CPU time (see [11,30,31] and some recent works [4,5,7,8,12,19,20,28], etc). Since non-overlapping methods have low computation and communication cost for each time step, they are preferable for large scale problems on massively parallel machines. Some explicit–implicit schemes on non-overlapping sub-domain decompositions have been proposed for parabolic equations to treat interface boundaries of sub-domains [9,13,21]. In [9], an explicit–implicit algorithm was developed, which relaxed the stability condition by using the larger spacing step size in the explicit scheme at the points of the interface boundaries of sub-domains. Paper [13] further proposed an explicit–implicit domain decomposition method for parabolic problems by using either a high-order explicit scheme or a multi-step explicit scheme on the interface which further relaxed the stability requirement. The methods in [9,13] work efficiently for stripe-divided sub-domains along one spatial variable for parabolic equations. However, on one aspect, it has been an important and difficult task to develop efficient explicit–implicit domain decomposition methods over multiple block-divided sub-domains so that it is more suitable and powerful to simulate large scale parabolic problems. On another aspect, there were few works to solve compressible fluid flows in porous media by applying explicit–implicit domain decomposition methods on non-overlapping sub-domains, which is also an important and challenging task for computing large scale fluid flows in porous media.

In this paper, we propose a new S-DDM iterative approach over multiple block-divided sub-domains for compressible contamination fluid flows in porous media by combining the non-overlapping domain decomposition, splitting, linearization and extrapolation techniques. In our method, the global domain is divided into multiple block sub-domains and is further partitioned into fine meshes on each sub-domain. At each time step, firstly the S-DDM scheme is proposed to solve the water head equation, in which we use an efficient local multilevel scheme to solve the values of water head on the interfaces of sub-domains and use the splitting implicit scheme to solve the interior values of water head in sub-domains. The proposed S-DDM overcomes the limitation of the stripe-divided sub-domains for parabolic equations in [9,13] and is an efficient and simple explicit–implicit domain decomposition method over multi-block sub-domains. Secondly, a S-DDM scheme combining the upstream volume technique is proposed to solve the concentration equation. In the S-DDM iterative approach, we also propose to combine the linearization and extrapolation techniques to treat the coupling and nonlinearity. Moreover, at each time step, an iterative process is applied for increasing the accuracy, which is controlled by a maximum iterative number and the desired accuracy. The proposed S-DDM iterative approach keeps the excellent advantages of the non-overlapping domain decompositions and the splitting technique. The efficient local multilevel schemes at interface points relax the stability condition of the S-DDM and improve the accuracy near the interface boundaries as well. The S-DDM iterative approach reduces computational complexities, large memory requirements and long computational durations, and is more suitable and powerful for parallel computing. Numerical experiments are taken for computing the problems of homogeneous flows, groundwater contaminations, and contaminations in concentration dependent density and in more general layered media. Numerical results show the efficient performance of the method for solving compressible contamination fluid flows in porous media. The proposed approach can be extended to solve high-dimensional large scale problems of fluid flows in porous media.

The paper is organized as follows. In Section 2, we introduce the mathematical model of compressible contamination fluid flows in porous media. In Section 3, we describe the S-DDM iterative approach for solving the coupling system of contamination fluid flows in porous media. In Section 4, numerical experiments are presented. Finally, some conclusions are addressed in Section 5.

2. Mathematical model of contamination fluid flows

For simulating contamination fluid flows, one first needs to build mathematical models to describe the processes of fluid flows in porous media [1,3,6,14]. In this section, we will derive the time-dependent partial differential equations governed by the mass conservations, the Darcy's law, and the equations of state in porous media.

2.1. Porous media and Darcy's law

Porous media are made up of cavities, or pores, surrounded by a solid matrix which may be for instance packed or consolidated grains. These kinds of media are filled with one or more fluids (see Fig. 1). The porosity of a porous medium, which describes the fraction of void space in the material, is defined by:

$$\phi = \frac{V_v}{V_T},$$

where V_v is the volume of void-space (such as fluids) and V_T is the total or bulk volume of material, including the solid and void components. Porosity is a fraction between 0 and 1, typically ranging from less than 0.01 for solid granite to more than 0.5 for peat and clay.

The Darcy's law establishes the basic relationship between the flow rate and the pressure gradient, which is the most widely used law or correlation in describing fluid flows in porous media. For the flow of water in vertical homogeneous sand filters, the famous Darcy's formula is

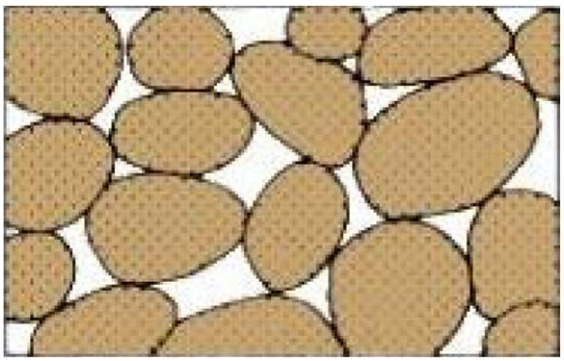

Fig. 1. An example of porous media [3].

$$\mathcal{Q} = KA(h_1 - h_2)/L,$$

which concludes that the rate of flow $\mathcal{Q}$ is proportional both to the constant cross-section area A and to $(h_1 - h_2)$ and inversely proportional to the length L, where h is the hydraulic head and $h_1 - h_2$ is the difference in hydraulic head across the filter of length L. Let $\mathbf{x} \in \Omega \subset \mathbf{R}^2$, and let ρ be the mass density of the fluid, p be the pressure, and the Darcy's velocity $\mathbf{u}(\mathbf{x}, t) = (u_x(\mathbf{x}, t), u_y(\mathbf{x}, t))^\tau$. The Darcy's law can be described as

$$\mathbf{u} = -\frac{\mathbf{k}}{\mu}(\nabla p + \rho g \nabla Z), \tag{2.1}$$

where g is the gravity constant, Z is the elevation height of the fluid measured from some chosen datum level [3]. $\mathbf{k}$ is the permeability tensor, given by

$$\mathbf{k} = \begin{pmatrix} k_{xx} & 0 \\ 0 & k_{yy} \end{pmatrix}, \tag{2.2}$$

which quantifies the ability of the porous medium domain to transmit a fluid. μ is the dynamical viscosity of the fluid. The porous medium is homogeneous if its permeability $\mathbf{k}$ is constant, otherwise, it is heterogeneous, e.g. the layered media.

2.2. The mass conservations

Let $A \subset \Omega$ be any representative volume element (REV). The conservation of mass states that the rate of mass accumulated within A equals the rate of mass injected into A across the boundary $\Gamma = \partial A$ of A plus the net amount of mass injected into A via sources and sinks. The conservation of mass for the fluid mixture can be expressed as

$$\frac{d}{dt}\int_A \phi\rho d\mathbf{x} = -\int_{\partial A} \rho\mathbf{u}\cdot\mathbf{n} ds + \int_A Q d\mathbf{x}, \quad \forall A \subset \Omega, \tag{2.3}$$

where $\mathbf{n} = (n_x, n_y)^\tau$ is the unit outward normal to Γ, and Q is the source and sink term that represents the mass flow rate per unit volume moving into or out the REV A. By the Gauss theorem, we obtain

$$\int_A \frac{\partial}{\partial t}(\phi\rho) d\mathbf{x} = \int_A (-\nabla\cdot(\rho\mathbf{u}) + Q) d\mathbf{x}, \quad \forall A \subset \Omega. \tag{2.4}$$

Further, we obtain the following partial differential form

$$\frac{\partial}{\partial t}(\phi\rho) = -\nabla\cdot(\rho\mathbf{u}) + Q, \quad \mathbf{x} \in \Omega, t \in (0, T]. \tag{2.5}$$

Let $c(\mathbf{x}, t)$ be the contaminant concentration of mass. The Fick's law states

$$\mathbf{J} = -\mathbf{D}\nabla c, \tag{2.6}$$

where $\mathbf{J}$ is the diffusion flux and $\mathbf{D}$ is the diffusion coefficient tensor, which describes the rate of diffusion of matter across a plane to be proportional to the negative of the rate of change of the concentration of the diffusing substance in the direction perpendicular to the plane. The conservation of mass for the contaminant states that the rate of mass accumulated within A equals the rate of mass flowing by the total (volumetric) flux plus the amount of mass diffused and dispersed and plus the net amount of mass injected into A via sources and sinks, which can be expressed as

$$\frac{d}{dt}\int_A \phi c d\mathbf{x} = -\int_{\partial A} (\mathbf{u}c - \mathbf{D}\nabla c)\cdot\mathbf{n} ds + \int_A Q c^* d\mathbf{x}, \quad \forall A \subset \Omega, \tag{2.7}$$

where $(\mathbf{u}c - \mathbf{D}\nabla c)$ is the total flux flowing into A across the boundary Γ of A. c^* is prescribed concentration at sources. By using the Gauss theorem, from (2.7), we can obtain the partial differential equation of solute concentration

$$\frac{\partial(\phi c)}{\partial t} + \nabla \cdot (\mathbf{u}c - \mathbf{D}\nabla c) = Qc^*, \quad \mathbf{x} \in \Omega, \ \ t \in (0, T]. \tag{2.8}$$

2.3. The water head and concentration coupling system

Due to the effect of the pressure changes, the porous media can be deformed [3,1]. Let c_ϕ be the compressibility of porous media, which is defined by

$$c_\phi = \frac{1}{\phi}\frac{\partial \phi}{\partial p}. \tag{2.9}$$

Integrating this equation gives,

$$\phi = \phi_0(\mathbf{x}) \exp(c_\phi(p - p_r)), \tag{2.10}$$

where $\phi_0(\mathbf{x})$ is the reference porosity of the medium at the reference pressure p_0. This result is widely used for modeling subsurface contaminant transport and re-mediation in the hydroscience community.

Let $s_p(\mathbf{x}, p)$ be the storage term, which is defined by

$$s_p(\mathbf{x}, p) = \frac{\partial(\phi\rho)}{\partial p} = \rho(p)\phi(\mathbf{x}, p)(c_\phi(\mathbf{x}) + c_\rho), \quad \mathbf{x} \in \Omega, \ \ t \in (0, T]. \tag{2.11}$$

Then, combining the equation of fluid flow (2.5), the Darcy's law and the equations of state, we get the equation for pressure p

$$s_p(\mathbf{x}, p)\frac{\partial p}{\partial t} + \nabla \cdot \rho\mathbf{u} = Q, \quad \mathbf{x} \in \Omega, \ \ t \in (0, T]. \tag{2.12}$$

In groundwater modeling, the water head is widely used, which is defined as (see [3])

$$\mathcal{H} = \int_{p_0}^{p} \frac{dp}{g\rho(p)} + Z. \tag{2.13}$$

In computation, the practical water head is defined as ([3,32,33], etc):

$$\mathcal{H} = \frac{p}{\rho_0 g} + Z, \tag{2.14}$$

where ρ_0 presents the density of reference water (fresh water). Since the compressibility of water is very small, it is possible to suppose that water is incompressible, i.e. ρ is only dependent of the concentration c. Here, the Hugakorn's linearization of density has

$$\rho = \rho_0\left(1 + \epsilon\frac{c}{c_s}\right), \tag{2.15}$$

where c_s is the concentration corresponding to the maximum density ρ_s and $\epsilon = (\rho_s - \rho_0)/\rho_0$ is the density ratio.

Using (2.9), (2.11), (2.14) and (2.15), we obtain the coupled system of water head and concentration equations:

$$\begin{cases} S_s\frac{\partial \mathcal{H}}{\partial t} - \nabla \cdot (\mathbf{K}(\nabla\mathcal{H} + \eta c\nabla Z)) = -\phi\eta\frac{\partial c}{\partial t} + \frac{Q}{\rho_0}, & \mathbf{x} \in \Omega, t \in (0, T], \\ \mathbf{u} = -\frac{\rho_0}{\rho}\mathbf{K}(\nabla\mathcal{H} + \eta c\nabla Z), & \mathbf{x} \in \Omega, t \in (0, T], \\ \phi\frac{\partial c}{\partial t} + \nabla \cdot (\mathbf{u}c - \mathbf{D}\nabla c) = Qc^* - \frac{\rho_0}{\rho}S_s\frac{\partial \mathcal{H}}{\partial t}c, & \mathbf{x} \in \Omega, t \in (0, T], \end{cases} \tag{2.16}$$

where $S_s = \rho\phi c_\phi g$ is the storage coefficient, $\mathbf{K} = \frac{\mathbf{k}\rho g}{\mu}$ is the hydraulic conductivity and $\eta = \epsilon/c_s$.

The problem is time-dependent, providing both initial and boundary conditions for water head $\mathcal{H}$ and concentration $c(\mathbf{x}, t)$. Let the boundary $\Gamma = \partial\Omega$ be composed of three parts Γ_1, Γ_2 and Γ_3 such that $\Gamma = \Gamma_1 \oplus \Gamma_2 \oplus \Gamma_3$. The proper Dirichlet boundary condition, Neumann boundary condition, or mixed boundary condition could be provided on Γ_1, Γ_2 or Γ_3. The initial conditions for water head and concentration are given as

$$\begin{aligned} &\mathcal{H}(\mathbf{x}, 0) = \mathcal{H}_0(\mathbf{x}), \quad \mathbf{x} \in \Omega, \\ &c(\mathbf{x}, 0) = c_0(\mathbf{x}), \quad \mathbf{x} \in \Omega. \end{aligned} \tag{2.17}$$

Remark 2.1. The system (2.16) of compressible contamination fluid flows in porous media is a nonlinearly coupled system of equations governed by the convection and diffusion processes, one is a parabolic equation of water head and the other is a convection–diffusion equation of concentration. This system is characterized by the nonlinearity, the coupling among these equations, the compressibility of the fluid and the medium, the enormous size of field-scale application, and the required long time period of prediction, numerical simulations of these systems encounter serious difficulties and complexities.

Remark 2.2. Domain decomposition methods (DDMs) allow the reduction of the sizes of problems by decomposing the domain into smaller ones on which the problems can be solved by multiple computers in parallel. The splitting technique is another method to reduce high-dimensional problems to a series of one-dimensional problems in each time interval. In the following section, we will develop a new efficient numerical method for solving multi-dimensional contamination fluid flows in porous media by combining the non-overlapping domain decomposition and the splitting technique.

3. The S-DDM iterative approach for contamination fluid flows

For simulating large scale fluid flows in porous media, we need to develop efficient domain decomposition methods for solving model (2.16). Since non-overlapping methods have low computation and communication cost for each time step, they are preferable for large scale problems. Papers [9,13] proposed explicit–implicit domain decomposition methods for parabolic equations by using either a high-order explicit scheme or a multi-step explicit scheme on the interface, which are efficient for stripe-divided sub-domains along one spatial variable. However, it has been an important and difficult task to develop efficient explicit–implicit domain decomposition methods over multiple block-divided sub-domains, and meanwhile, there were few works to solve the compressible fluid flows in porous media by applying the methods, which is important and challenging for powerfully simulating large scale fluid flows problems. In this section, we propose a new S-DDM iterative approach over multiple block-divided sub-domains by combining non-overlapping domain decompositions and the splitting technique for the coupled system of water head and concentration equations.

We consider two dimensional problems on $\Omega = [a_x, b_x] \times [a_z, b_z]$. The problem (2.16) can be rewritten in the operator form

$$\begin{cases} S_s \frac{\partial \mathcal{H}}{\partial t} + \mathcal{L}_{\mathcal{H}x}(c)\mathcal{H} + \mathcal{L}_{\mathcal{H}z}(c)\mathcal{H} = \delta(c) + f(\mathcal{H}, c), \\ u_x = -\frac{\rho_0 K_x}{\rho}\frac{\partial \mathcal{H}}{\partial x}, \quad u_z = -\frac{\rho_0 K_z}{\rho}\left(\frac{\partial \mathcal{H}}{\partial z} + \eta c\right), \\ \phi \frac{\partial c}{\partial t} + \mathcal{L}_{cx}(\mathcal{H})c + \mathcal{L}_{cz}(\mathcal{H})c = g(\mathcal{H}, c), \end{cases} \tag{3.1}$$

where the operators are defined as

$$\mathcal{L}_{\mathcal{H}x}(c)\mathcal{H} = -\frac{\partial}{\partial x}\left(K_x(c)\frac{\partial \mathcal{H}}{\partial x}\right), \quad \mathcal{L}_{\mathcal{H}z}(c)\mathcal{H} = -\frac{\partial}{\partial z}\left(K_z(c)\frac{\partial \mathcal{H}}{\partial z}\right), \tag{3.2}$$

$$\mathcal{L}_{cx}(\mathcal{H})c = \frac{\partial (u_x c)}{\partial x} - \frac{\partial}{\partial x}\left(D_x(\mathcal{H})\frac{\partial c}{\partial x}\right), \quad \mathcal{L}_{cz}(\mathcal{H})c = \frac{\partial (u_z c)}{\partial z} - \frac{\partial}{\partial z}\left(D_z(\mathcal{H})\frac{\partial c}{\partial z}\right), \tag{3.3}$$

and $\mathbf{u} = (u_x, u_z)^\tau$ is the Darcy's velocity, $\mathbf{K} = diag(K_x, K_z)$ is the hydraulic conductivity and $\mathbf{D} = diag(D_x, D_z)$ is the diffusion coefficient tensor. The functions in the right hand side are

$$\delta(c) = \frac{\partial (K_z(c)\eta c)}{\partial z}, \quad f(\mathcal{H}, c) = -\phi(\mathcal{H})\eta\frac{\partial c}{\partial t} + \frac{Q}{\rho_0}, \tag{3.4}$$

$$g(\mathcal{H}, c) = Qc^* - \frac{\rho_0 S_s(c)}{\rho(c)}\frac{\partial \mathcal{H}}{\partial t}c, \tag{3.5}$$

where Q is the source, and we assume that

$$f = f_1 + f_2, \quad g = g_1 + g_2. \tag{3.6}$$

Problem (3.1) is subject to some proper initial and boundary conditions prescribed as in Section 2.

3.1. Partition and domain decomposition

We divide the large domain Ω into $d = N_r \times N_s$ multiple block sub-domains $\Omega_{r,s}$. Each $\Omega_{r,s}$ is further partitioned into fine meshes by using step size h, see Figs. 2 and 3.

In general, the number d of sub-domains is related to the size of the real problem. The sub-domains may have different lengths and different step sizes in different sub-domains, which may be determined by the local behavior of the problem.

Let us introduce, for example, a uniform four block-divided mesh Ω_h as the tensor direct product of $I_h \times J_h$ of one-dimensional mesh, $I_h = \{a_x = x_0, x_1, \ldots, x_r, \ldots, x_{I-1},\ x_I = b_x\}$ and $J_h = \{a_z = z_0, z_1, \ldots, z_s, \ldots, z_{J-1},\ z_J = b_z\}$, where $x = x_r$ and $z = z_s$ are interface boundaries of sub-domains which divide Ω into four sub-domains $\Omega_{l,q},\ l, q = 1, 2$. Further, for general uniform block-divided domain decomposition, we denote IN_r to be the index number of interface points along x-direction and IN_s to be the index number of interface points along z-direction. On each sub-domain $\Omega_{r,s}$, we denote I_r to be the index number of mesh points along x-direction and J_s to be the index number of mesh points along z-direction. Then, we denote the spatial step sizes by $h_x = \frac{1}{I}$ and $h_z = \frac{1}{J}$ along x-direction and z-direction, respectively. We introduce the notations: $x_{i+\frac{1}{2}} = \frac{x_i + x_{i+1}}{2},\ z_{j+\frac{1}{2}} = \frac{z_j + z_{j+1}}{2},\ x_{-\frac{1}{2}} = x_0,\ x_{I+\frac{1}{2}} = x_I,\ z_{-\frac{1}{2}} = z_0,\ z_{J+\frac{1}{2}} = z_J$.

Denote positive integer N to be the number of time steps. We then define a time partition:

$$0 = t^0 < t^1 < \cdots < t^n < \cdots < t^{N-1} < t^N = T, \tag{3.7}$$

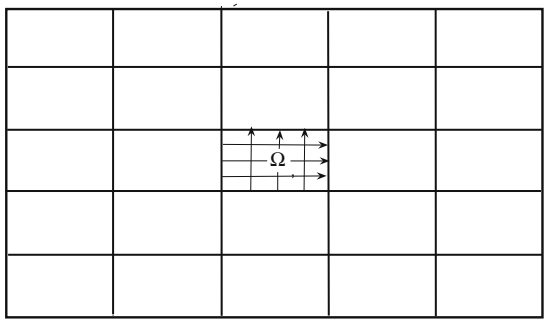

Fig. 2. The domain Ω and sub-domains $\Omega_{r,s}$.

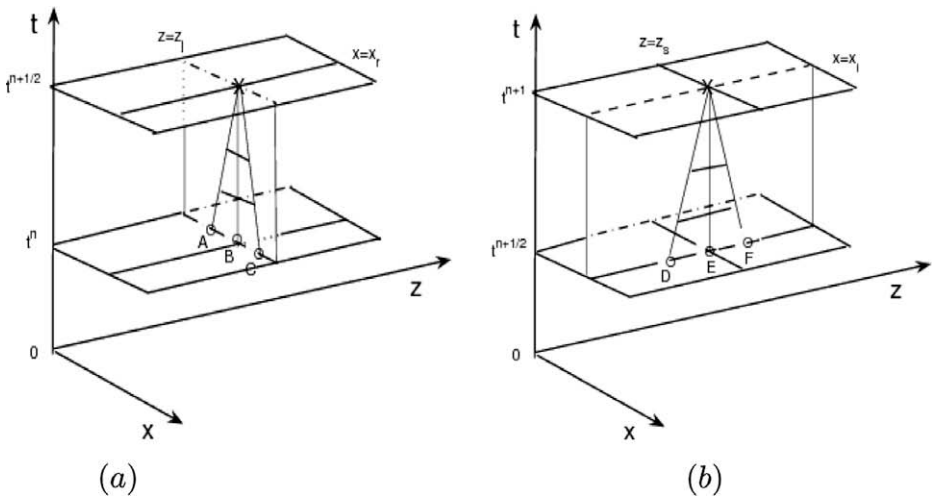

Fig. 3. (a) The first half step from $t^n \to t^{n+\frac{1}{2}}$ along x-direction. $x = x_r$ is the interface of sub-domains. For $0 < j < J$, the point A is (x_{r-K}, z_j) and point B is (x_r, z_j) and point C is (x_{r+K}, z_j). (b) The second half step from $t^{n+\frac{1}{2}} \to t^{n+1}$ along z-direction. $z = z_s$ is the interface of sub-domains. For $0 < i < I$, the point D is (x_i, z_{s-K}) and point E is (x_i, z_s) and point F is (x_i, z_{s+K}).

where $\Delta t^n = t^n - t^{n-1}$, for $n = 1, 2, \ldots, N$, are the time steps. For a function $w(x, z, t)$, we define $w^n_{i,j} = w(x_i, z_j, t^n)$ at mesh point (x_i, z_j, t^n). Then, we denote $w^n_{hi,j}$ to be the approximation solution to $w^n_{i,j}$ at mesh point (x_i, z_j, t^n).

In order to further define the numerical scheme in the following subsection, we now introduce the time semi-discretization solution $(\widetilde{\mathcal{H}}^n,\ \tilde{c}^n)$ for all $n \geqslant 0$. Set $\widetilde{\mathcal{H}}^0 = \mathcal{H}_0(x, z)$ and $\tilde{c}^0 = c_0(x, z)$. For $n \geqslant 0$, in each time interval $(t^n, t^{n+1}]$, the semi-discretization solution $(\widetilde{\mathcal{H}}^{n+1},\ \tilde{c}^{n+1})$ satisfies

$$\begin{cases} \big(S_s(\bar{c}^{n+1}))I + \Delta t \mathcal{L}_{\mathcal{H}x}(\bar{c}^{n+1})\big)\widetilde{\mathcal{H}}^{n+\frac{1}{2}} = \widetilde{\mathcal{H}}^n + \Delta t \bar{f}_1^{n+1}, \\ \big(S_s(\bar{c}^{n+1}))I + \Delta t \mathcal{L}_{\mathcal{H}z}(\bar{c}^{n+1})\big)\widetilde{\mathcal{H}}^{n+1} = \widetilde{\mathcal{H}}^{n+\frac{1}{2}} + \Delta t(\bar{\delta}^{n+1} + \bar{f}_2^{n+1}), \end{cases} \tag{3.8}$$

and

$$\begin{cases} \Big(\phi(\widetilde{\mathcal{H}}^{n+1})I + \Delta t \mathcal{L}_{cx}(\widetilde{\mathcal{H}}^{n+1})\Big)\tilde{c}^{n+\frac{1}{2}} = \tilde{c}^n + \Delta t \bar{g}_1^{n+1}, \\ \Big(\phi(\widetilde{\mathcal{H}}^{n+1})I + \Delta t \mathcal{L}_{cz}(\widetilde{\mathcal{H}}^{n+1})\Big)\tilde{c}^{n+1} = \tilde{c}^{n+\frac{1}{2}} + \Delta t \bar{g}_2^{n+1}, \end{cases} \tag{3.9}$$

subject to proper boundary and initial conditions. In the scheme, $\overline{\mathcal{H}}^{n+1}$ and $\bar{c}^{n+1}$ are the approximation solutions $\widetilde{\mathcal{H}}^n$ and $\tilde{c}^n$ at time $t = t^n$ or the extrapolating approximations of previous level values at $t = t^n$ and $t = t^{n-1}$; and $\bar{\delta}^{n+1} = \delta(\bar{c}^{n+1})$, $\bar{f}_l = f_l(\overline{\mathcal{H}}^{n+1}, \bar{c}^{n+1})$, $\bar{g}_l = g_l(\widetilde{\mathcal{H}}^{n+1}, \bar{c}^{n+1})$, for $l = 1, 2$. We will evaluate $\bar{c}^{n+1}$ and $\overline{\mathcal{H}}^{n+1}$ later in this paper.

3.2. The S-DDM scheme for the water head equation

We first construct the splitting domain decomposition scheme for the water head equation in time interval $(t^n, t^{n+1}]$ where $n \geqslant 0$.

For the interior points of sub-domains, we define the discrete operators $\mathcal{L}_{\mathcal{H}x,h_x}(w)$ and $\mathcal{L}_{\mathcal{H}z,h_z}(w)$ to be the discretization of the operators $\mathcal{L}_{\mathcal{H}x}(c)$ and $\mathcal{L}_{\mathcal{H}z}(c)$ by the implicit scheme on I_h and J_h, respectively, i.e., for each $z_j \in J_h$,

$$\mathcal{L}_{\mathcal{H}x,h_x}(w)\mathcal{H}^n_{i,j} \equiv \frac{1}{h_x^2}\Big(-K_{xi-\frac{1}{2}j}(w)\mathcal{H}^n_{i-1,j} + \Big(K_{xi-\frac{1}{2}j}(w) + K_{xi+\frac{1}{2}j}(w)\Big)\mathcal{H}^n_{i,j} - K_{xi+\frac{1}{2}j}(w)\mathcal{H}^n_{i+1,j}\Big). \tag{3.10}$$

Similarly, for each $x_i \in I_h$,

$$\mathcal{L}_{\mathcal{H}z,h_z}(w)\mathcal{H}^n_{i,j} \equiv \frac{1}{h_z^2}\Big(-K_{zi,j-\frac{1}{2}}(w)\mathcal{H}^n_{i,j-1} + \Big(K_{zi,j-\frac{1}{2}}(w) + K_{zi,j+\frac{1}{2}}(w)\Big)\mathcal{H}^n_{i,j} - K_{zi,j+\frac{1}{2}}(w)\mathcal{H}^n_{i,j+1}\Big), \tag{3.11}$$

where w is a function.

For the interface points, we define a local multilevel explicit scheme. Let $\Delta\tau^n = \Delta t^n/K$ be the multilevel time step by further dividing the time level $[t^n, t^{n+1}]$ into K subintervals on the interfaces, and let $\hat{h}_q = mh_q,\ q = x, z$, be the spatial step size related to interfaces, where $K \geqslant 1$ and $m \geqslant 1$ are integer numbers. Let $\tau^k_n = k\Delta\tau^n$. For a function w, we define $w^{n,k}_{i,j} = w(x_i, z_j, t^n + \tau^k_n)$ at grid point $(x_i, z_j, t^n + \tau^k_n)$. We denote $w^{n,k}_{hi,j}$ to be the numerical approximation to $w^{n,k}_{i,j}$. Then, for the interface points $x_r, r \in IN_r$ and $z_s, s \in IN_s$, we define the discrete operators $\mathcal{L}_{\mathcal{H}x,\hat{h}_x}(w)$ and $\mathcal{L}_{\mathcal{H}z,\hat{h}_z}(w)$ to be the approximations to the operators $\mathcal{L}_{\mathcal{H}x}(c)$ and $\mathcal{L}_{\mathcal{H}z}(c)$ with step size $\hat{h}_x$ and $\hat{h}_z$, respectively. For each $z_j \in J_h$, at point (x_{r_l}, z_j), where $r_l = r, r \pm m, \ldots, r \pm Km,\ r \in IN_r$, we let

$$\mathcal{L}_{\mathcal{H}x,\hat{h}_x}(w)\mathcal{H}^{n,k-1}_{r_l,j} \equiv \frac{1}{\hat{h}_x^2}\Big(-K_{xr_l-m+\frac{1}{2}j}(w)\mathcal{H}^{n,k-1}_{r_l-m,j} + \Big(K_{xr_l-m+\frac{1}{2}j}(w) + K_{xr_l+m-\frac{1}{2}j}(w)\Big)\mathcal{H}^{n,k-1}_{r_l,j} - K_{xr_l+m-\frac{1}{2}j}(w)\mathcal{H}^{n,k-1}_{r_l+m,j}\Big), \tag{3.12}$$

and for each $x_i \in I_h$, at point $(x_i, z_{s_l}),\ s_l = s, s \pm m, \ldots, s \pm Km,\ s \in IN_s$,

$$\mathcal{L}_{\mathcal{H}z,\hat{h}_z}(w)\mathcal{H}^{n,k-1}_{i,s_l} \equiv \frac{1}{\hat{h}_z^2}\Big(-K_{zi,s_l-m+\frac{1}{2}}(w)\mathcal{H}^{n,k-1}_{i,s_l-m} + \Big(K_{zi,s_l-m+\frac{1}{2}}(w) + K_{zi,s_l+m-\frac{1}{2}}(w)\Big)\mathcal{H}^{n,k-1}_{i,s_l} - K_{zi,s_l+m-\frac{1}{2}}(w)\mathcal{H}^{n,k-1}_{i,s_l+m}\Big). \tag{3.13}$$

With the notations and formulas above, we now propose our splitting domain decomposition method (S-DDM) for the water head equation in time interval $(t^n, t^{n+1}]$ as follows. Let $\bar{c}^{n+1}_h$ be the founded approximation to concentration $c(t^{n+1})$ which will be defined in Section 3.4.

Firstly along x-direction, $\forall j \in J_s,\ s \in IN_s$

(a) the local multilevel explicit scheme is defined on interface points for finding the interface values $\mathcal{H}^{n+\frac{1}{2}}_{hr,j}$ for $r \in IN_r$. By setting,

$$\mathcal{H}^{n,0}_{hr_l,j} = \mathcal{H}^n_{hr_l,j}, \quad r_l = r, r \pm m, \ldots, r \pm Km;\ \ r \in IN_r, \tag{3.14}$$

and for $k = 1, 2, \ldots, K$, computing

$$\mathcal{H}^{n,k}_{hr_l,j} = \Big(S_{sr_l,j}(\bar{c}^{n+1}_h)I - \Delta\tau\mathcal{L}_{\mathcal{H}x,\hat{h}_x}(\bar{c}^{n+1}_h)\Big)\mathcal{H}^{n,k-1}_{hr_l,j} + \Delta\tau\bar{f}^{n+1}_{1r_l,j}, \quad r_l = r, r \pm m, \ldots, r \pm Km;\ \ r \in IN_r, \tag{3.15}$$

then we set $\mathcal{H}^{n+\frac{1}{2}}_{hr,j} = \mathcal{H}^{n,K}_{hr,j}$ for $r \in IN_r$;

(b) after getting the interface values above, the implicit x-directional splitting scheme is defined to find the interior point values on each sub-domain, by solving

$$(S_{si,j}(\bar{c}^{n+1}_h)I + \Delta t\mathcal{L}_{\mathcal{H}x,h_x}(\bar{c}^{n+1}_h))\mathcal{H}^{n+\frac{1}{2}}_{hi,j} = \mathcal{H}^n_{hi,j} + \Delta t\bar{f}^{n+1}_{1i,j}, i \in I_r, r \in IN_r. \tag{3.16}$$

Secondly, along z-direction, $\forall i \in I_r,\ r \in IN_r$

(c) the interface values $\mathcal{H}^{n+1}_{hi,s}$, at points z_s for $s \in IN_s$, are computed by the local multilevel explicit scheme. Setting

$$\mathcal{H}^{n+1,0}_{hi,s_l} = \mathcal{H}^{n+\frac{1}{2}}_{hi,s_l}, \quad s_l = s, s \pm m, \ldots, s \pm Km;\ \ s \in IN_s, \tag{3.17}$$

and for $k = 1, 2, \ldots K$, computing

$$\mathcal{H}^{n+\frac{1}{2},k}_{hi,s_l} = (S_{si,s_l}(\bar{c}^{n+1}_h)I - \Delta\tau\mathcal{L}_{\mathcal{H}z,\hat{h}_z}(\bar{c}^{n+1}_h))\mathcal{H}^{n+\frac{1}{2},k-1}_{hi,s_l} + \Delta\tau\bar{\delta}^{n+1}_{i,j} + \Delta\tau\bar{f}^{n+1}_{2i,s_l}, \quad s_l = s,\ \ s \pm m, \ldots, s \pm Km;\ \ s \in IN_s, \tag{3.18}$$

then we let $\mathcal{H}^{n+1}_{hi,s} = \mathcal{H}^{n+\frac{1}{2},K}_{hi,s}$ for $s \in IN_s$;

(d) the interior point values of sub-domains are solved by the implicit z-direction splitting scheme:

$$\big(S_{si,j}(\bar{c}^{n+1}_h)I + \Delta t\mathcal{L}_{\mathcal{H}z,h_z}(\bar{c}^{n+1}_h)\big)\mathcal{H}^{n+1}_{hi,j} = \mathcal{H}^{n+\frac{1}{2}}_{hi,j} + \Delta t\bar{\delta}^{n+1}_{i,j} + \Delta t\bar{f}^{n+1}_{2i,j}, \quad j \in J_s,\ \ s \in IN_s. \tag{3.19}$$

Scheme (3.14)–(3.19) constructs the S-DDM on multiple block-divided sub-domains for computing the water head $\mathcal{H}^{n+1}_h$ at $t = t^{n+1}$.

Further, we compute the Darcy's velocity $U^{n+1} = (U_x^{n+1}, U_z^{n+1})^\tau$ at $t = t^{n+1}$. For all $z_j \in J_h$,

$$U_{xi+\frac{1}{2}j}^{n+1} = \frac{\rho_0}{h_x}\left[\frac{\overline{K}_x}{\bar{\rho}}\right]_{i+\frac{1}{2}j}^{n+1}\left(\mathcal{H}_{hi+1\,j}^{n+1} - \mathcal{H}_{hij}^{n+1}\right), \quad i \in I_r,\ \ r \in IN_r, \tag{3.20}$$

and for all $x_i \in I_h$,

$$U_{zij+\frac{1}{2}}^{n+1} = \frac{\rho_0}{h_z}\left[\frac{\overline{K}_z}{\bar{\rho}}\right]_{ij+\frac{1}{2}}^{n+1}\left((\mathcal{H}_{hij+1}^{n+1} - \mathcal{H}_{hij}^{n+1}) + \eta h_z \bar{c}_{hij+\frac{1}{2}}^{n+1}\right), \quad j \in J_s,\ \ s \in IN_s, \tag{3.21}$$

where $\overline{K}_{xi+\frac{1}{2}j}^{n+1} = K_x\left(\bar{c}_{hi+\frac{1}{2}j}^{n+1}\right)$, $\overline{K}_{zij+\frac{1}{2}} = K_z\left(\bar{c}_{hij+\frac{1}{2}}^{n+1}\right)$, $\bar{\rho}_{i+\frac{1}{2}j}^{n+1} = \rho\left(\bar{c}_{hi+\frac{1}{2}j}^{n+1}\right)$, $\bar{\rho}_{ij+\frac{1}{2}}^{n+1} = \rho\left(\bar{c}_{hij+\frac{1}{2}}^{n+1}\right)$, and $\bar{c}_{hij+\frac{1}{2}}^{n+1} = \frac{1}{2}\left(\bar{c}_{hij}^{n+1} + \bar{c}_{hij+1}^{n+1}\right)$.

Remark 3.1. In this subsection, we have proposed a new splitting domain decomposition method (S-DDM) to approximate the water head at $t = t^{n+1}$ on multiple block-divided sub-domains by combining the non-overlapping domain decomposition and the splitting technique. Our S-DDM scheme overcomes the limitation of strip-divided sub-domains in [9,13] for the linear parabolic equations. The S-DDM scheme can work efficiently over multiple block-divided sub-domains. On each block-divided sub-domain, the two dimensional water head equation has been split into uncoupled one-dimensional problems. In each time interval, we first solved the interface values of the solution by a local multilevel explicit scheme on the interface boundaries of sub-domains and then solved the interior solutions in interiors of sub-domains by the splitting implicit scheme. The local multilevel scheme at interface points can relax the stability condition and improve the accuracy near the interface boundaries as well.

3.3. The S-DDM scheme for the concentration equation

Then, we propose the S-DDM scheme by combining the upstream volume technique for the concentration equation in time interval $(t^n, t^{n+1}]$ where $n \geqslant 0$.

At the interior points of sub-domains, we define the discrete operators $\mathcal{L}_{cx,h_x}(\mathcal{H}_h)$ and $\mathcal{L}_{cz,h_z}(\mathcal{H}_h)$ to approximate the operators $\mathcal{L}_{cx}(\mathcal{H})$ and $\mathcal{L}_{cz}(\mathcal{H})$ by using the upstream volume technique on I_h and J_h, respectively.

For a given $z_j \in J_h$, we have the following approximation for $x = x_i$:

$$\frac{\partial(u_x^{n+1}c^{n+1})}{\partial x}(x_i, z_j) \approx \frac{1}{h_x}\left(u_{xi+\frac{1}{2}j}^{n+1}c_{i+\frac{1}{2}j}^{n+1} - u_{xi-\frac{1}{2}j}^{n+1}c_{i-\frac{1}{2}j}^{n+1}\right). \tag{3.22}$$

In order to avoid the nonphysical numerical oscillations, we combine the upstream volume technique. We define function $\omega(x)$ as:

$$\omega(x) = \begin{cases} 1, & x \geqslant 0, \\ 0, & x < 0. \end{cases}$$

Then, we have the equality:

$$u_{xi+\frac{1}{2}j}^{n+1}c_{i+\frac{1}{2}j}^{n+1} = u_{xi+\frac{1}{2}j}^{n+1}\left(\omega\left(u_{xi+\frac{1}{2}j}^{n+1}\right)c_{i+\frac{1}{2}j}^{n+1} + \left(1 - \omega\left(u_{xi+\frac{1}{2}j}^{n+1}\right)\right)c_{i+\frac{1}{2}j}^{n+1}\right),$$

where $\omega(u_{xi+\frac{1}{2}j}^{n+1})$ and $(1 - \omega(u_{xi+\frac{1}{2}j}^{n+1}))$ refer to the positive and negative transport velocities, respectively. Noting the approximation U^{n+1} of velocity u^{n+1}, we define the following approximation from (3.22),

$$\frac{\partial(u_x^{n+1}c^{n+1})}{\partial x}(x_i, z_j) \approx \frac{1}{h_x}\left(-\beta_{xi-1\,j}^{n+1}c_{i-1\,j}^{n+1} + \beta_{xij}^{n+1}c_{ij}^{n+1} - \beta_{xi+1\,j}^{n+1}c_{i+1\,j}^{n+1}\right), \tag{3.23}$$

where

$$\beta_{xi-1\,j}^{n+1} = U_{xi-\frac{1}{2}j}^{n+1}\omega(U_{xi-\frac{1}{2}j}^{n+1}), \quad \beta_{xi+1\,j}^{n+1} = U_{xi+\frac{1}{2}j}^{n+1}\left(1 - \omega\left(U_{xi+\frac{1}{2}j}^{n+1}\right)\right),$$
$$\beta_{xij}^{n+1} = U_{xi+\frac{1}{2}j}^{n+1}\omega\left(U_{xi+\frac{1}{2}j}^{n+1}\right) + U_{xi-\frac{1}{2}j}^{n+1}\left(1 - \omega\left(U_{xi-\frac{1}{2}j}^{n+1}\right)\right).$$

For the second derivative term of $\mathcal{L}_{cx}(\mathcal{H})$, we use the central volume approximation:

$$-\frac{\partial}{\partial x}(D_x(\mathcal{H}^{n+1})\frac{\partial c^{n+1}}{\partial x})(x_i, z_j) \approx \frac{1}{h_x^2}\left\{-D_{xi-\frac{1}{2}j}(\mathcal{H}_h^{n+1})c_{i-1\,j}^{n+1} + \left(D_{xi-\frac{1}{2}j}(\mathcal{H}_h^{n+1}) + D_{xi+\frac{1}{2}j}(\mathcal{H}_h^{n+1})\right)c_{ij}^{n+1} - D_{xi+\frac{1}{2}j}(\mathcal{H}_h^{n+1})c_{i+1\,j}^{n}\right\}. \tag{3.24}$$

Now, from (3.23) and (3.24), we can define the discrete operator $\mathcal{L}_{cx,h_x}(\mathcal{H}_h^{n+1})$ to $\mathcal{L}_{cx}(\mathcal{H}^{n+1})$ as: $\forall z_j \in J_h$,

$$\mathcal{L}_{cx,h_x}(\mathcal{H}_h^{n+1})c_{ij}^{n+1} \equiv \frac{1}{h_x^2}\left(-\beta_{xi-1\,j}^{(n+1)*}c_{i-1\,j}^{n+1} + \beta_{xij}^{(n+1)*}c_{ij}^{n+1} - \beta_{xi+1\,j}^{(n+1)*}c_{i+1\,j}^{n+1}\right), \tag{3.25}$$

where

$$\beta^{(n+1)*}_{xi-1,j} = \beta^{n+1}_{xi-1,j} + D_{xi-\frac{1}{2},j}(\mathcal{H}^{n+1}_h), \quad \beta^{(n+1)*}_{xi+1,j} = \beta^{n+1}_{xi+1,j} + D_{xi+\frac{1}{2},j}(\mathcal{H}^{n+1}_h),$$
$$\beta^{(n+1)*}_{xi,j} = \beta^{n+1}_{xi,j} + D_{xi-\frac{1}{2},j}(\mathcal{H}^{n+1}_h) + D_{xi+\frac{1}{2},j}(\mathcal{H}^{n+1}_h).$$

Repeating the procedure of (3.22)–(3.24) for the z-direction, we can define the discrete operator $\mathcal{L}_{cz,h_z}(\mathcal{H}^{n+1}_h)$ to $\mathcal{L}_{cz}(\mathcal{H}^{n+1})$, $\forall x_i \in I_h$,

$$\mathcal{L}_{cz,h_z}(\mathcal{H}^{n+1}_h)c^{n+1}_{i,j} \equiv \frac{1}{h_z^2}\left(-\beta^{(n+1)*}_{zi,j-1}c^{n+1}_{i,j-1} + \beta^{(n+1)*}_{zi,j}c^{n+1}_{i,j} - \beta^{(n+1)*}_{zi,j+1}c^{n+1}_{i,j+1}\right), \tag{3.26}$$

where

$$\beta^{(n+1)*}_{zi,j-1} = U^{n+1}_{zi,j-\frac{1}{2}}\omega\left(U^{n+1}_{zi,j-\frac{1}{2}}\right) + D_{zi,j-\frac{1}{2}}(\mathcal{H}^{n+1}_h),$$
$$\beta^{(n+1)*}_{zi,j+1} = U^{n+1}_{zi,j+\frac{1}{2}}\left(1-\omega\left(U^{n+1}_{zi,j+\frac{1}{2}}\right)\right) + D_{zi,j+\frac{1}{2}}(\mathcal{H}^{n+1}_h),$$
$$\beta^{(n+1)*}_{zi,j} = U^{n+1}_{zi,j+\frac{1}{2}}\omega\left(U^{n+1}_{zi,j+\frac{1}{2}}\right) + U^{n+1}_{zi,j-\frac{1}{2}}\left(1-\omega\left(U^{n+1}_{zi,j-\frac{1}{2}}\right)\right) + D_{zi,j-\frac{1}{2}}(\mathcal{H}^{n+1}_h) + D_{zi,j+\frac{1}{2}}(\mathcal{H}^{n+1}_h).$$

Then, for the interface points of sub-domains, we define the discrete operators $\mathcal{L}_{cx,\hat{h}_x}(\mathcal{H}^{n+1}_h)$ and $\mathcal{L}_{cz,\hat{h}_z}(\mathcal{H}^{n+1}_h)$ to approximate the operators $\mathcal{L}_{cx}(\mathcal{H}^{n+1})$ and $\mathcal{L}_{cy}(\mathcal{H}^{n+1})$ with spatial step sizes $\hat{h}_q$, $q = x, z$. For each $z_j \in J_h$, at points (x_{r_l}, z_j), $r_l = r, r \pm m, \ldots, r \pm Km$, $r \in IN_r$, let

$$\mathcal{L}_{cx,\hat{h}_x}(\mathcal{H}^{n+1}_h)c^{n,k-1}_{r_l,j} \equiv \frac{1}{\hat{h}_x^2}\left(-\beta^{(n+1)*}_{xr_l-m,j}c^{n,k-1}_{r_l-m,j} + \beta^{(n+1)*}_{xr_l,j}c^{n,k-1}_{r_l,j} - \beta^{(n+1)*}_{xr_l+m,j}c^{n,k-1}_{i+1,j}\right), \tag{3.27}$$

and at points (x_i, z_{s_l}), $s_l = s, s \pm m, \ldots, s \pm Km$, $s \in IN_s$, let

$$\mathcal{L}_{cz,\hat{h}_z}(\mathcal{H}^{n+1}_h)c^{n,k-1}_{i,s_l} \equiv \frac{1}{\hat{h}_z^2}\left(-\beta^{(n+1)*}_{zi,s_l-m}c^{n,k-1}_{i,s_l-m} + \beta^{(n+1)*}_{zi,s_l}c^{n,k-1}_{i,s_l} - \beta^{(n+1)*}_{zi,s_l+m}c^{n}_{i,s_l+m}\right). \tag{3.28}$$

With the definitions of the discrete operators above, the S-DDM scheme for the concentration equation is defined as follows.

Firstly along x-direction, $\forall j \in J_s$, $s \in IN_s$

(a) the local multilevel explicit scheme is defined for finding the interface values $c^{n+1}_{hr,j}$, $r \in IN_r$. Setting

$$c^{n,0}_{hr_l,j} = c^{n}_{hr_l,j}, \quad r_l = r, r \pm m, \ldots, r \pm Km; \ r \in IN_r, \tag{3.29}$$

and for $k = 1, 2, \ldots, K$, computing

$$c^{n,k}_{hr_l,j} = \left(\phi_{r_l,j}(\mathcal{H}^{n+1}_h)I - \Delta\tau\mathcal{L}_{cx,\hat{h}_x}(\mathcal{H}^{n+1}_h)\right)c^{n,k-1}_{hr_l,j} + \Delta\tau\bar{g}^{n+1}_{1r_l,j}, \quad r_l = r, r \pm m, \ldots, r \pm Km; \ r \in IN_r, \tag{3.30}$$

where $\Delta\tau$ is the local multilevel time step, and then we set $c^{n+\frac{1}{2}}_{h\ r,j} = c^{n,K}_{hr,j}$ for $r \in IN_x$;

(b) after getting the interface values, the implicit x-directional splitting scheme on each sub-domain is defined to find the interior point values $c^{n+\frac{1}{2}}_h$, by solving tri-diagonal systems

$$\left(\phi_{i,j}(\mathcal{H}^{n+1}_h)I + \Delta t\mathcal{L}_{cx,h_x}(\mathcal{H}^{n+1}_h)\right)c^{n+\frac{1}{2}}_{hi,j} = c^{n}_{hi,j} + \Delta t\bar{g}^{n+1}_{1i,j}, \quad i \in I_r, \ r \in IN_r. \tag{3.31}$$

Secondly, along z-direction, $\forall i \in I_r$, $r \in IN_r$

(c) the values at the interface points are computed by the local multilevel explicit scheme by setting

$$c^{n+1,0}_{hi,s_l} = c^{n+\frac{1}{2}}_{hi,s_l}, \quad s_l = s, s \pm m, \ldots, s \pm Km; \ s \in IN_s, \tag{3.32}$$

and for $k = 1, 2, \ldots K$, computing

$$c^{n+\frac{1}{2},k}_{hi,s_l} = \left(\phi_{i,s_l}(\mathcal{H}^{n+1}_h)I - \Delta\tau\mathcal{L}_{cz,\hat{h}_z}(\mathcal{H}^{n+1}_h)\right)c^{n+\frac{1}{2},k-1}_{hi,s_l} + \Delta\tau\bar{g}^{n+1}_{2i,s_l}, \quad s_l = s, s \pm m, \ldots, s \pm Km; \ s \in IN_s, \tag{3.33}$$

and then letting $c^{n+1}_{hi,s} = c^{n+\frac{1}{2},K}_{hi,s}$ for $s \in IN_s$, where $\Delta\tau$ is the local multilevel time step;

(d) the interior point values of sub-domains are solved by the implicit z-directional splitting scheme on each sub-domain:

$$\left(\phi_{i,j}(\mathcal{H}^{n+1}_h)I + \Delta t\mathcal{L}_{cz,h_z}(\mathcal{H}^{n+1}_h)\right)c^{n+1}_{hi,j} = c^{n+\frac{1}{2}}_{hi,j} + \Delta t\bar{g}^{n+1}_{2i,j}, \quad j \in J_s, \ s \in IN_s. \tag{3.34}$$

Scheme (3.29)–(3.34) defines the S-DDM on multiple sub-domains to find the approximations c_h^{n+1} for the concentration equation at time $t = t^{n+1}$.

Remark 3.2. For the concentration equation, we have defined the S-DDM scheme by combining the upstream volume technique. The developed S-DDM scheme can also be used by combining high order upstream volume techniques, for example, the optimal weighted upstream covolume method in [22] for increasing the accuracy, and the methods can also be applied by combining other efficient techniques of treating convection terms.

3.4. The S-DDM iterative approach

Finally, we can propose the S-DDM iterative approach for solving the coupled system (3.1) of contamination fluid flows in porous media. To describe the iterative algorithm, we define the following notations of approximation by using the extrapolation technique. Let $q \geqslant 0$ be the index of the linearization iteration number for treating the coupled nonlinearity. For $q = 0$, we define

$$F(\bar{w}^{n,0})(x,z) = \begin{cases} w^{n-1}(x,z), & n = 1, \\ (1+\frac{\Delta t^n}{\Delta t^{n-1}})w^{n-1}(x,z) - \frac{\Delta t^n}{\Delta t^{n-1}} w^{n-2}(x,z), & 2 \leqslant n \leqslant N, \end{cases} \tag{3.35}$$

and for $q \geqslant 1$, we define

$$F(\bar{w}^{n,q})(x,z) = \begin{cases} w^{n,0}(x,z), & q = 1, \\ (1-\theta)w^{n,q-2}(x,z) + \theta w^{n,q-1}(x,z), & q \geqslant 2. \end{cases} \tag{3.36}$$

where the function w^n can be the water head $\mathcal{H}_h^n$ or the concentration c_h^n, and $0 < \theta < 2$ is a weighting parameter for the iterative procedure.

For the functions $\delta(c)$, $f(\mathcal{H},c)$ and $g(\mathcal{H},c)$, we propose the following approximations, for $n \geqslant 0$, at any point (i,j) and $q \geqslant 0$:

$$\delta(\bar{c}_{i,j}^{n,q}) = \begin{cases} \frac{\eta}{h_z}\left(K_z(\bar{c}_{i,j}^{n,q})\bar{c}_{i,j}^{n,q} - K_z(\bar{c}_{i,j-m}^{n,q})\bar{c}_{i,j-m}^{n,q}\right), & z_j = z_s,\ s \in IN_s, \\ \frac{\eta}{h_z}\left(K_z(\bar{c}_{i,j}^{n,q})\bar{c}_{i,j}^{n,q} - K_z(\bar{c}_{i,j-1}^{n,q})\bar{c}_{i,j-1}^{n,q}\right), & z_j \neq z_s,\ s \in IN_s, \end{cases} \tag{3.37}$$

$$f(\overline{\mathcal{H}}_{i,j}^{n,q}, \bar{c}_{i,j}^{n,q}) = \begin{cases} \phi(\bar{\mathcal{H}}_{i,j}^{n,q})\eta\bar{c}_{i,j}^{nq} + Q_{i,j}^n/\rho_0, & n = 0, \\ \frac{\phi(\bar{\mathcal{H}}_{i,j}^{n,q})\eta}{\Delta t}\left(\bar{c}_{i,j}^{n,q} - c_{i,j}^{n-1}\right) + Q_{ij}^n/\rho_0, & n \geqslant 1, \end{cases} \tag{3.38}$$

$$g(\overline{\mathcal{H}}_{i,j}^{n,q}, \bar{c}_{i,j}^{n,q}) = \begin{cases} \frac{\rho_0 S_s(\bar{c}_{i,j}^{n,q})\bar{c}_{i,j}^{n,q}}{\rho_{i,j}^{n,q}(\bar{c})}\overline{\mathcal{H}}_{i,j}^{n,q} + Q_{i,j}^n c_{i,j}^*, & n = 0, \\ \frac{\rho_0 S_s(\bar{c}_{i,j}^{n,q})\bar{c}_{i,j}^{n,q}}{\rho(\bar{c}_{i,j}^{n,q})\Delta t}\left(\overline{\mathcal{H}}_{i,j}^{n,q} - \mathcal{H}_{i,j}^{n-1}\right) + Q_{i,j}^n c_{i,j}^*, & n \geqslant 1. \end{cases} \tag{3.39}$$

We may use the decompositions of functions $f_1 = f_2 = \frac{1}{2}f$ and $g_1 = g_2 = \frac{1}{2}g$. Let $q_0 \geqslant 0$ be the maximum number of linearization iteration, let $N > 0$ be the maximum number of time levels, and let K be the maximum number of local multilevels for interface values.

Now, we describe the algorithm of our S-DDM iterative approach for contamination fluid flows in porous media as follows:

The algorithm of the S-DDM iterative approach:

Step 1. **Initialization:** Set $\mathcal{H}_{hi,j}^0 = \mathcal{H}_0(x_i, z_j)$, $c_{hi,j}^0 = c_0(x_i, z_j)$, for any (i,j).
Step 2. **Time Stepping Procedure:** for $0 \leqslant n \leqslant N-1$, do steps 3–13:
Step 3. Set $\mathcal{H}_{hr_l,j}^{n,0} = \mathcal{H}_{hr_l,j}^n$ and $c_{hr_l,j}^{n,0} = c_{hr_l,j}^n$, for $r_l = r, r \pm m, \ldots, r \pm Km,\ r \in IN_r,\ \forall j \in J_s, J_s \in IN_s$.
Step 4. **Iteration Step:** for $0 \leqslant q \leqslant q_0$, do steps 5–11:
Step 5. (**Compute water head**) Along x-direction, for $j \in J_s,\ s \in IN_s$:

(a) For $k = 1, 2 \ldots, K$, find the interface values by local multilevel explicit scheme with $\mathcal{H}_{hr_l,j}^{n,q,0} = \mathcal{H}_{hr_l,j}^{n,q}$, $r_l = r, r \pm m, \ldots, r \pm Km,\ r \in IN_r$, and

$$\mathcal{H}_{hr_l,j}^{n,q,k} = (S_s(F_{r_l,j}(\bar{c}_h^{n+1,q}))I - \Delta\tau\mathcal{L}_{\mathcal{H}x,\hat{h}_x}(F_{r_l,j}(\bar{c}_h^{n+1,q})))\mathcal{H}_{hr_l,j}^{n,q,k-1} + \Delta\tau f_1(F_{r_l,j}(\overline{\mathcal{H}}_h^{n+1,q}), F_{r_l,j}(\bar{c}_h^{n+1,q})). \tag{3.40}$$

(b) Set $\mathcal{H}_{hr,j}^{n+\frac{1}{2},q} = \mathcal{H}_{hr,j}^{n,q,K},\ r \in IN_r$.

(c) Find the interior values in sub-domains by splitting implicit scheme

$$(S_s(F_{i,j}(\bar{c}_h^{n+1,q}))I + \Delta t\mathcal{L}_{\mathcal{H}x,h_x}(F_{i,j}(\bar{c}_h^{n+1,q})))\mathcal{H}_{hi,j}^{n+\frac{1}{2},q} = \mathcal{H}_{hi,j}^n + \Delta t f_1(F_{i,j}(\overline{\mathcal{H}}_h^{n+1,q}), F_{i,j}(\bar{c}_h^{n+1,q})), \quad i \in I_r,\ r \in IN_r. \tag{3.41}$$

Step 6. Along z-direction, $\forall x_i \in I_r,\ r \in IN_r$:

(a) For $k = 1, 2 \ldots, K$, find the interface values by local multilevel explicit scheme with $\mathcal{H}^{n+\frac{1}{2},q,0}_{hi,s_l} = \mathcal{H}^{n+\frac{1}{2},q}_{hi,s_l},\ s_l = s, s\pm m, \ldots, s \pm Km,\ s \in IN_s$, and

$$\mathcal{H}^{n+\frac{1}{2},q,k}_{hi,s_l} = (S_s(F_{i,s_l}(\bar{c}^{n+1,q}_h)) - \Delta\tau\mathcal{L}_{\mathcal{H}z,\hat{h}_z}(F_{i,s_l}(\bar{c}^{n+1,q}_h)))\mathcal{H}^{n+\frac{1}{2},q,k-1}_{hi,s_l} + \Delta\tau\delta(F_{i,s_l}(\bar{c}^{n+1,q}_h)) + \Delta\tau f_2(F_{i,s_l}(\overline{\mathcal{H}}^{n+1,q}_h), F_{i,s_l}(\bar{c}^{n+1,q}_h)). \tag{3.42}$$

(b) Set $\mathcal{H}^{n+1,q}_{hi,s} = \mathcal{H}^{n+\frac{1}{2},q,K}_{hi,s},\ s \in IN_s$.

(c) Find the interior values in sub-domains by splitting implicit scheme

$$(S_s(F_{i,j}(\bar{c}^{n+1,q}_h))I + \Delta t\mathcal{L}_{\mathcal{H}z,h_z}(F_{i,j}(\bar{c}^{n+1,q}_h)))\mathcal{H}^{n+1,q}_{hi,j} = \mathcal{H}^{n}_{hi,j} + \Delta t\delta(F_{i,j}(\bar{c}^{n+1,q}_h)) + \Delta t f_2(F_{i,j}(\overline{\mathcal{H}}^{n+1,q}_h), F_{i,j}(\bar{c}^{n+1,q}_h)),\ j \in I_s,\ s \in IN_s. \tag{3.43}$$

Step 7. Evaluate the x-directional component of velocity for $j \in J_s,\ s \in IN_s$:

$$U^{n+1,q}_{xi+\frac{1}{2}j} = \frac{\rho_0 K_x\left(F_{i+\frac{1}{2}j}(\bar{c}^{n+1,q}_h)\right)}{\rho\left(F_{i+\frac{1}{2}j}(\bar{c}^{n+1,q}_h)\right)h_x}(\mathcal{H}^{n+1,q}_{hi+1,j} - \mathcal{H}^{n+1,q}_{hi,j}),\quad i \in I_r,\ r \in IN_r, \tag{3.44}$$

and the z-directional component of the velocity for $i \in I_r,\ r \in IN_r$:

$$U^{n+1,q}_{zi,j+\frac{1}{2}} = \frac{\rho_0 K_z\left(F_{i,j+\frac{1}{2}}(\bar{c}^{n+1,q}_h)\right)}{\rho\left(F_{i,j+\frac{1}{2}}(\bar{c}^{n+1,q}_h)\right)h_z}\{(\mathcal{H}^{n+1,q}_{hi,j+1} - \mathcal{H}^{n+1,q}_{hi,j}) + \eta h_z F_{i,j+\frac{1}{2}}(\bar{c}^{n+1,q}_h)\},\quad j \in J_s,\ s \in IN_s. \tag{3.45}$$

Step 8. (**Compute concentration**) Along x-direction, for $j \in J_s,\ s \in IN_s$:

(a) For $k = 1, 2 \ldots, K$, find the interface values by local multilevel explicit scheme with $c^{n,q,0}_{hr_l j} = c^{n,q}_{hr_l j},\ r_l = r, r \pm m, \ldots, r \pm Km,\ r \in IN_r$,

$$c^{n,q,k}_{hr_l j} = (\phi_{r_l j}(\mathcal{H}^{n+1,q}_h)I - \Delta\tau\mathcal{L}_{cx,\hat{h}_x}(\mathcal{H}^{n+1,q}_h))c^{n,k-1(q)}_{hr_l j} + \Delta\tau g_1(\mathcal{H}^{n+1,q}_{hr_l j}, F_{r_l j}(\bar{c}^{n+1,q}_h)). \tag{3.46}$$

(b) Set $c^{n+\frac{1}{2},q}_{hr,j} = c^{n,q,K}_{hr,j},\ r \in IN_r$.

(c) Find the interior values in sub-domains by implicit scheme

$$(\phi_{i,j}(\mathcal{H}^{n+1,q}_h)I + \Delta t\mathcal{L}_{cx,h_x}(\mathcal{H}^{n+1,q}_h))c^{n+\frac{1}{2},q}_{hi,j} = c^{n}_{hi,j} + \Delta t g_1(\mathcal{H}^{n+1,q}_{hi,j}, F_{i,j}(\bar{c}^{n+1,q}_h)),\quad i \in I_r,\ r \in IN_r. \tag{3.47}$$

Step 9. Along z-direction, for $i \in I_r,\ r \in IN_r$, similar with Step 6, find $c^{n+1,q}_{hi,j},\ j \in J_s,\ s \in IN_s$.

Step 10. Calculate $Err_1 = \|\mathcal{H}^{n+1,q}_h - \mathcal{H}^{n+1,q-1}_h\|$ and $Err_2 = \|c^{n+1,q}_h - c^{n+1,q-1}_h\|$.

Step 11. **If** $\max\{Err1, Err2\} \leqslant$ Tolerance, then **goto** Step 12.
else Set $q = q + 1$.
end if

Step 12. Set $\mathcal{H}^{n+1}_{hi,j} = \mathcal{H}^{n+1,q}_{hi,j},\ c^{n+1}_{hi,j} = c^{n+1,q}_{hi,j}$ for any (i,j).

Step 13. Set $n = n + 1$.

Step 14. Output $\mathcal{H}^{N}_{hi,j}$ and $c^{N}_{hi,j},\ \forall(i,j)$.
Stop.

Remark 3.3. In the S-DDM iterative approach, the large domain Ω is divided into multiple block sub-domains. At each time step, we firstly compute the approximate water head and the approximate velocity, and then find the approximate concentration by a linearization procedure. For solving either the water head equation or the concentration equation, we compute the interface values by the local multilevel explicit scheme or the local multilevel explicit scheme combined with the upstream volume technique on interface boundaries of sub-domains, and compute the interior solutions in sub-domains by the splitting implicit scheme or the splitting implicit scheme combining the upstream volume technique, respectively. The local multilevel schemes at interfaces are just multilevel explicit schemes which can be solved directly. The slitting implicit schemes lead to symmetric and tri-diagonal algebraic systems on sub-domains which can be easily solved by the Thomas' algorithm. The local multilevel explicit schemes at interface points can relax the stability condition and improve the accuracy near the interface boundaries. Keeping the advantages of the non-overlapping domain decomposition method and the splitting technique, the developed S-DDM iterative approach reduces computational complexities, large memory requirements and long computational durations.

Remark 3.4. Since the model of contamination fluid flows in porous media is the coupled nonlinear system, in the proposed S-DDM iterative approach we apply the linearization technique and the extrapolation technique to treat the coupling and the nonlinearity. Moreover, at each time step, a linearization iterative process is applied in the S-DDM approach for increasing the accuracy, which is controlled by the maximum iterative number q_0 and the desired accuracy (*tolerance*). The linearization iteration here is for increasing the accuracy and meanwhile the S-DDM approach still works even without iteration ($q_0 = 1$) (i.e. a linearization scheme). A reasonable tolerance will be expected in computation. The looping of time steps will always

Table 1
The effect of K on the stability.

$\lambda^* =$	8.2		4. 1		2.05		1.025		0.5125	
K	L_∞	L_2	L_∞	L_2	L_∞	L_2	L_∞	L_2	L_∞	L_2
1	div	div	div	div	div	div	1.304e−3	8.249e−4	1.658e−3	1.113e−3
4	div	div	div	div	7.750e−4	4.964e−4	1.301e−3	8.228e−4	1.659e−3	1.114e−3
10	div	div	2.656e−3	1.497e−3	7.900e−4	4.993e−4	1.303e−3	8.244e−4	1.660e−3	1.114e−3
16	7.090e−3	4.234e−3	2.651e−3	1.494e−3	7.930e−4	4.997e−4	1.304e−3	8.248e−4	1.660e−3	1.114e−3

Table 2
The effect of m on the stability.

$\lambda^* =$	8.2		4.1		2.05		1.025		0.5125	
m	L_∞	L_2	L_∞	L_2	L_∞	L_2	L_∞	L_2	L_∞	L_2
1	div	div	div	div	div	div	1.304e−3	8.249e−4	1.658e−3	1.113e−3
2	div	div	2.516e−3	1.391e−3	9.210e−4	5.570e−4	1.501e−3	9.574e−4	1.894e−3	1.256e−3
3	6.663e−3	3.880e−3	2.317e−3	1.237e−3	2.317e−3	1.237e−3	1.951e−3	1.241e−3	2.387e−3	1.553e−3
4	6.365e−3	3.613e−3	2.002e−3	1.062e−3	1.821e−3	1.105e−3	2.680e−3	1.679e−3	3.140e−3	2.003e−3

work and will go to next time step when q reaches to the max number q_0, if it does not meet the tolerance condition. In any case, the iteration improves the accuracy. As we use a local multilevel scheme on interfaces of sub-domains, K and m have made actually no condition with respect to Δt and h by proper $K > 1$ and $m > 1$, since the stability condition $\lambda = \frac{\Delta\tau}{h^2}(D + |V|\hat{h}/2) = \frac{1}{Km^2}\lambda^* \leqslant \frac{1}{2}$, where $\lambda^* = \frac{\Delta t}{h^2}(D + |V|mh/2)$, is always true with respect to Δt and h for proper $K > 1$ and $m > 1$. Numerical results are shown in Tables 1 and 2 in the following section. Though it is developed for two dimensional problem in this section, the S-DDM iterative approach can be extended to solve high-dimensional porous media flows.

Remark 3.5. Our S-DDM technique proposed in this section develops an efficient approach over non-overlapping multiple block sub-domains, which is more suitable and powerful for parallel computing and for large scale simulation of compressible contamination flows in porous media. The splitting implicit schemes used in each sub-domain will provide reasonable accuracy and reduce the computational costs. The local multilevel schemes used in the interfaces of sub-domains will improve the stability and accuracy near the interfaces of sub-domains. We have noted that for solving accurately the solution near the fracture in the fractured porous flows, paper [27] proposed an implicit sub-time stepping method to use sub-time stepping in the fracture domain. The local sub-time step refining can efficiently improve the accuracy when simulating flow and transport in fractured porous media. Thus, for further studying fractured media flows, our S-DDM technique can be applied, by combining the sub-time stepping in the sub-domains that contain the fractures, to solve the large scale fluid flows in fractured media for parallel computing, which will be a very interesting future work.

4. Numerical experiments

In this section, we present numerical experiments for compressible contamination fluid flows in porous media to illustrate the performance of the S-DDM iterative approach. We firstly study homogenous flows and focus on studying the stability, accuracy and efficiency of the S-DDM approach by presenting the stability, error, ratio of convergence, and CPU time. Then, we consider the groundwater contamination problems where the contamination is loaded on the boundary. Finally, we will carry out simulations of the groundwater contamination problems where the density depends on concentration and in more general layered media.

4.1. Homogenous flows

We consider the following homogeneous flow

$$\begin{cases} \frac{\partial \mathcal{H}}{\partial t} - \nabla(\mathbf{D}_{\mathcal{H}}\mathcal{H}) = 0, & (x,y) \in \Omega,\ \ t \in (0,T], \\ \mathbf{v} = -\mathbf{D}_{\mathcal{H}}\nabla\mathcal{H}, & (x,y) \in \Omega,\ \ t \in (0,T], \\ \frac{\partial c}{\partial t} + \nabla\cdot(\mathbf{v}c) - \nabla(\mathbf{D}_c\nabla c) = 0, & (x,y) \in \Omega,\ \ t \in (0,T], \end{cases}$$

where $\Omega = [a_x, b_x] \times [a_y, b_y]$, which is horizontal; $\partial\Omega_1 = \{x = a_x\} \times [a_y, b_y] \oplus \{x = b_x\} \times [a_y, b_y]$, and $\partial\Omega_2 = \{y = a_y\} \times [a_x, b_x] \oplus \{y = b_y\} \times [a_x, b_x]$. $\mathbf{v} = (V_x, V_y)^\tau$ is the Darcy's velocity field. $\mathbf{D}_{\mathcal{H}} = diag(D_{\mathcal{H}x}, D_{\mathcal{H}y})$ is the hydraulic conductivity. $\mathbf{D}_c = diag(D_{cx}, D_{cy})$ is the diffusion coefficient. The boundary conditions are $\mathcal{H}(x,y,t) = g_{in}(x,y,t),\ (x,y) \in \partial\Omega_1,\ \ \mathbf{v}\cdot\mathbf{n} = g_{out}(x,y,t), (x,y) \in \partial\Omega_2,\ c(x,y,t) = h_{in}(x,y,t), (x,y) \in \partial\Omega_1,\ -\mathbf{D}_c\nabla c(x,y,t)\cdot\mathbf{n} = h_{out}(x,y,t),\ (x,y) \in \partial\Omega_2$, where $g_{in}, g_{out}, h_{in}, h_{out}$ are specified functions. The initial values are given as $H(x,y,0) = H_0(x,y)$ and $c(x,y,0) = c_0(x,y)$.

We first investigate the stability of the S-DDM for the concentration equation on domain $\Omega = [0,1] \times [0,1]$. The initial value $c_0(x,y) = 0$. The inflow boundary h_{in} equals to 1 at $x = 0$ and 0 at $x = 1$ for all y. The computation is taken on 2×2 subdomains. Let diffusion coefficients $D_{cx} = D_{cy} = 1$ and the velocity components $V_x = V_y = 1$. The step sizes are chosen as $h = 1/40$, and $\Delta t = 1/200$, 1/400, 1/800, 1/1600, 1/3200. For the local multilevel explicit scheme at interfaces of sub-domains, we take $\hat{h} = mh$ and $\Delta\tau = \Delta t/K$. We study the effect of the parameters K and m on the stability. The numerical results at $t = 0.1$ are presented in Tables 1 and 2. In Table 1 where $m = 1$, from the first row (K=1), we can see that when $\lambda^* = \frac{\Delta t}{h^2}(D + |\mathbf{v}|h/2) > 1.025$, i.e. the stability condition is broken, the standard explicit is divergent. However, if we use the local multilevel explicit scheme ($K \geqslant 4$) at the interfaces, the S-DDM works very well. For example, when $K = 16$ in the last row, even for $\lambda^* = 8.2$, we can still obtain accurate results where the error is 7.090×10^{-3} in the maximal norm. Similarly, in Table 2 where $K = 1$, we can relax the stability condition by increasing the value of m. For example, for $\lambda^* = 8.2$, if taking $m = 4$, the S-DDM method obtains the accurate approximation, the error 6.365×10^{-3} in maximal norm. As a local multilevel scheme on interfaces of sub-domains is used, K and m make the stability condition $\lambda = \frac{\Delta\tau}{\hat{h}^2}(D + |V|\hat{h}/2) = \frac{1}{Km^2}\lambda^* \leqslant \frac{1}{2}$ is always true with respect to Δt and h for proper $K > 1$ and $m > 1$, where $\lambda^* = \frac{\Delta t}{h^2}(D + |V|mh/2)$.

Then, we numerically study the convergence of the S-DDM approach for the concentration equation. The reference solution is solved by the S-DDM on fine meshes $h = 1/240$ and $\Delta t = 1/20,000$. To obtain the ratio of convergence in space, we fix the time step size $\Delta t = 1/6000$ and change the spatial step size h from 1/10 to 1/80. The diffusion coefficients are $D_{cx} = D_{cy} = 0.1$. We consider three different velocity fields with $V_x = 0, 1$ and 10, and $V_y = 0$. The errors at $t = 0.1$ and ratios of convergence are presented in Table 3. From Table 3, we can see that when $V_x = 0$ and $V_y = 0$, the ratio of convergence is second order in space while when $V_x = 1$ and 10, and $V_y = 0$, the ratio is first order due to the upstream volume method in the S-DDM approach for the convection term. To improve the accuracy and convergence ratio, a modified upstream covolume technique ([22]) can be applied to our S-DDM scheme.

Further, we analyze numerically the mass balance errors and their ratio in time step. Consider the problem with $c(x,y,0) = \sin^2(\pi x)\sin^2(\pi y)$ and with no flow boundary condition. First, let the diffusion coefficients $D_{cx} = D_{cy} = 0.1$ and the velocity $\mathbf{v} = (0,0)^\tau$. We choose $K = 2$ and $m = 2$ for the S-DDM. The time and space step sizes are chosen such that the ratio $\frac{\Delta t}{h^2} = 1$. The solution errors, mass balance errors and their ratios in time are presented in Table 4 for time $t = 0.5$. For computing the solution errors, the reference solution is obtained by the splitting finite difference method with very fine mesh $h = \frac{1}{240}$and $\Delta t = \frac{1}{10,000}$. From the table, we can see clearly that the convergence rate of mass balance errors is of first order in time and is higher than the ration of solution errors.

Then, take diffusion coefficients $D_{cx} = D_{cy} = 0.001$ and the velocity $\mathbf{v} = (V_x, 0)^\tau$ with $V_x = 0.5, 0.8$ and 1.0. We choose $K = 4$ and $m = 2$ for the S-DDM approach. The space and time step sizes are chosen such that $\Delta x = \Delta y$ and the ratio $\Delta t/\Delta x = 2$. The mass errors and ratios in time are presented in Table 5 for time $t = 0.2$. It clearly shows that the ratios of mass balance errors for different velocity components are still of first order in time.

Table 3
The errors and ratios in space for the problem with diffusion coefficients $D_{cx} = D_{cy} = 0.1$.

$\Delta x = \Delta y$		1/10	1/20	1/40	1/80
	L_∞-error	1.1780e−2	3.2900e−3	8.4500e−4	2.1300e−4
$V_x = 0$	Ratio	–	1.8402	1.9611	1.9881
$V_y = 0$	L_2-error	5.1214e−3	1.3448e−3	3.4541e−4	9.8252e− 5
	Ratio	–	1.9291	1.9610	1.8138
	L_∞-error	8.2925e−2	4.2031e−2	1.9843e−2	8.0490e−3
$V_x = 1$	Ratio	–	0.9804	1.0828	1.3017
$V_y = 0$	L_2-error	3.7573e−2	1.8784e−2	8.7427e−3	3.5284e−3
	Ratio	–	1.0002	1.1034	1.3091
	L_∞-error	1.4778e−1	1.0946e−1	9.3392e−2	5.2239e−2
$V_x = 10$	Ratio	–	0.4330	0.2290	0.8382
$V_y = 0$	L_2-error	7.6620e−2	5.3767e−2	3.3515e−2	1.7357e−2
	Ratio	–	0.5110	0.6819	0.9493

Table 4
The solution errors, mass balance errors and their ratios in time of the S-DDM approach for the diffusion problem with $D_{cx} = D_{cy} = 0.1$.

	Δt	1/100	1/400	1/1600	1/6400
	L_∞-error	2.1770e−2	3.6570e−3	6.7700e−4	1.1400e−4
Solution error	Ratio in time	–	1.2868	1.2167	1.2851
	L_2-error	7.7905e−3	1.3626e−3	2.6161e−4	4.5312e−5
	Ratio in time	–	1.2916	1.1565	1.2649
Mass error		5.7147e−3	7.4457e−4	9.3875e−5	1.1758e−5
	Ratio in time	–	1.4710	1.4938	1.4985

Table 5
The mass balance errors and ratios in time of the S-DDM approach for the problem with diffusion coefficients $D_{cx} = D_{cy} = 0.001$ and velocity $\mathbf{v} = (V_x, 0)^\tau$.

	Δt	1/30	1/40	1/50	1/60	1/70	1/80
$V_x = 0.5$	Mass error	3.7254e−3	2.5496e−3	1.8921e−3	1.4756e−3	1.1907e−3	9.8517e−4
	Ratio in time	–	1.3182	1.3369	1.3635	1.3916	1.4189
$V_x = 0.8$	Mass error	6.3064e−3	4.6914e−3	3.7140e−3	3.0474e−3	2.5618e−3	2.1928e−3
	Ratio in time	–	1.0283	1.0469	1.0852	1.1259	1.1648
$V_x = 1.0$	Mass error	8.2350e−3	6.3050e−3	5.1182e−3	4.2869e−3	3.6658e−3	3.1832e−3
	Ratio in time	–	0.9283	0.9346	0.9722	1.0152	1.0571

Table 6
The effect of K and m on CPU time.

	Δt	$\Delta x = \Delta y$	L_∞	L_2	CPU time (s)
$K = 1,\ m = 1$	$\frac{1}{2000}$	$\frac{1}{40}$	3.477e−3	1.899e−3	0.45
$K = 2,\ m = 1$	$\frac{1}{860}$	$\frac{1}{40}$	3.290e−3	1.280e−3	0.20
$K = 3,\ m = 1$	$\frac{1}{660}$	$\frac{1}{40}$	2.539e−3	1.250e−3	0.15
$K = 2,\ m = 2$	$\frac{1}{500}$	$\frac{1}{40}$	3.563e−3	1.469e−3	0.11
$K = 3,\ m = 2$	$\frac{1}{400}$	$\frac{1}{40}$	4.798e−3	1.876e−3	0.08

Moreover, we study the efficiency of the S-DDM approach. We will observe the consumed CPU time by the S-DDM approach. All computations and measurements are taken on a DELL poweredge server 2800 with Dual 3.2G Xeon CPU and 2G memory. We consider a concentration problem in variable velocity field $\mathbf{v} = (4\sin(\pi y), 0)^\tau$. Take the spatial step size $\Delta x = \Delta y = 1/40$ and the time step size from $\Delta t = 1/2000$ to $\Delta t = 1/400$. The numerical results at $t = 0.1$ are presented in Table 6. From the table, we observe that with proper parameters of K and m, we can reduce the consumed CPU time while keeping the similar accuracy. For example, in the first row with $K = 1$ and $m = 1$, the error in L_2-norm is 1.899e−3 and the CPU time is 0.45 s. If we use $K = 3$ and $m = 2$ in the last row, the S-DDM keeps the similar accuracy but greatly reduces the CPU time where the maximum error is 1.876e−3 while the CPU time is only 0.08 second. It's also worth to mention that in the case of $\Delta t = 1/400,\ h = 1/40$, without the multilevel scheme on the interface boundaries, the standard explicit scheme is divergent since the stability condition is broken.

Now, we show the numerical shape of the homogenous flow with a given velocity field $\mathbf{v} = (1, 0)^\tau$. The initial value $c_0(x, y) = 0$. The spatial step is $h = 1/20$ and the time step is $\Delta t = 1/100$. The parameters of the multilevel scheme are taken to be $K = 2,\ m = 2$. Firstly, let's look at the following case. At the inflow boundary, the concentration h_{in} is zero but $h_{in} = 1$ for $0.3 \leqslant y \leqslant 0.4$ and $0.6 \leqslant y \leqslant 0.7$. The outflow boundary conditions as well as the initial values are all set to be zero. In Fig. 4, we present the contour plots of concentration for four pair diffusion coefficients $(D_{cx}, D_{cy}) = (1, 1), (0.1, 0.1)$, (0.01, 0.01) and (0.1, 0) at time t = 0.01, 0.1 and 0.4. For $D_{cx} = D_{cy} = 1$, the stability condition of standard explicit scheme has been broken, where $\lambda^* = \frac{\Delta t}{h^2}(\max\{D_{cx}, D_{cy}\} + |\mathbf{v}|h/2) = 4.1$. From Fig. 4(a), we can see that the S-DDM scheme still works well for this case due to the application of multilevel scheme for the explicit scheme on interfaces. In this example, the nonzero concentration at the inflow boundary will move along the flow due to convection and diffusion. From Fig. 4(a) and (b), we observe that the concentration is propagating faster along x-direction than along y-direction since the velocity of the fluid along y-direction is zero. We can also see that when the diffusion coefficients decrease from 1 to 0.001, the convection dominates the transport process. For the special case with diffusion coefficient $D_{cy} = 0$ the concentration moves only along x-direction, as shown in Fig. 4(c).

We then consider the case that g_{in} is zero but $g_{in} = 1$ for $0.45 \leqslant y \leqslant 0.55$. Note that the nonzero part of the boundary condition is crossing the interface of the sub-domain, $y = 0.5$. The numerical results for $D_{cx} = D_{cy} = 1, 0.1$, and 0.01 at time $t = 0.01,\ 0.1$, and 0.4 are presented in Fig. 5. We can see that the approximation to the interface of sub-domains does not affect the shape of the solution, which indicates that the S-DDM treats the problem with nonzero concentration distribution on interface very well. Again, when the convection term dominates the diffusion term, in Fig. 5(c), it shows clearly that the propagation of the concentration mainly moves along the direction of the velocity.

As the last part of this subsection, we consider the coupled system of water head equation and concentration equation. The inflow boundary condition of water head $g_{in} = 40\sin(\pi y)$ at $x = 0$. The inflow boundary value of concentration is $h_{in} = 1$ at $x = 0$. The outflow boundary and initial values are chosen to be zero for both water head equation and concentration equation. The hydraulic conductivity and the diffusion coefficients are $D_{\mathcal{H}x} = D_{\mathcal{H}y} = 0.01$ and $D_{cx} = D_{cy} = 0.01$, respectively. The spatial and time step sizes are $h = /120$ and $\Delta t = 1/20$. We choose the parameters $K = 2$ and $m = 2$ for multilevel explicit scheme. The numerical results are shown in Fig. 6. The propagating process is presented at three time periods, $t = 0.01,\ 0.1$ and 0.4. From Fig. 6(a), we can see that the water head has bigger values at the middle $y = 0.5$ than those near upper and bottom boundaries. The velocity decreases from the middle $y = 0.5$ to the boundaries $y = 0$ and $y = 1$. Thus, the concentration spreads faster at $y = 0.5$ along x-direction, as shown in Fig. 6(b).

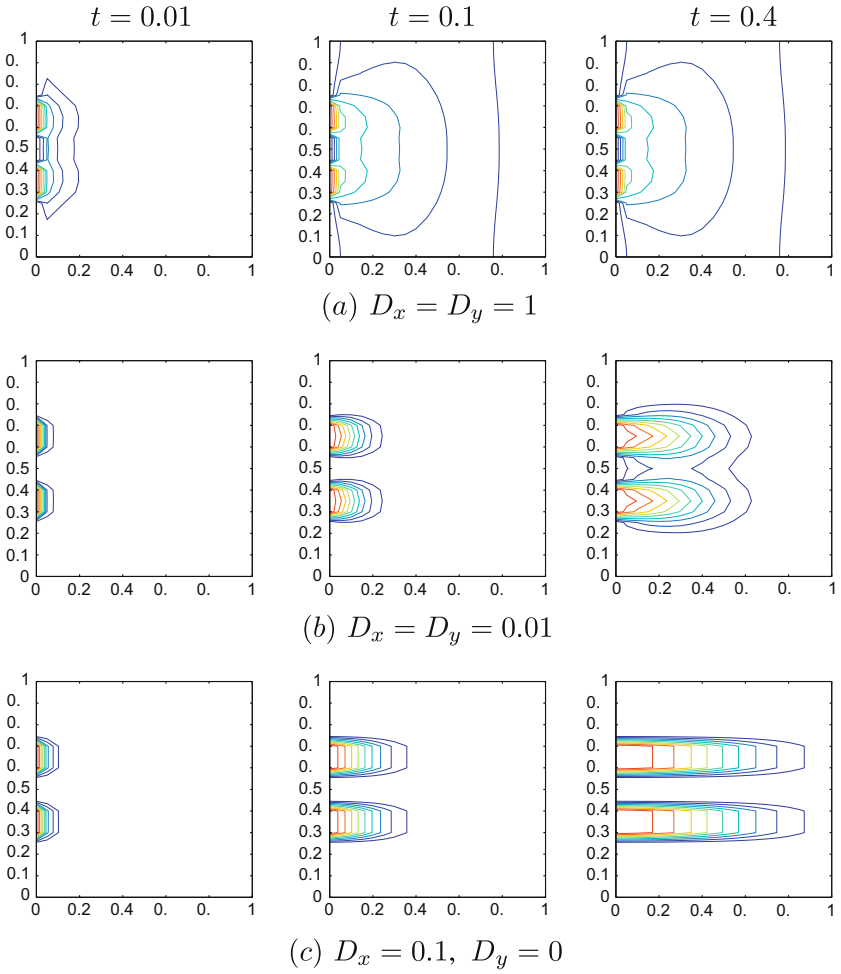

Fig. 4. The contour plots of the concentration in homogenous flows with different diffusion coefficients in a velocity field $\mathbf{v} = (1, 0)^{\tau}$.

4.2. Groundwater contaminations

In recent years, the growth of industry, technology, population, and water use has increased the stress upon groundwater. The quality of groundwater has been degraded. Industrial discharges, urban activities, agriculture, ground-water pumpage, and disposal of waste all can affect ground-water quality, for example, the Babylon landfill leachate. The contaminates in groundwater are usually composed of common ions like Na^+, Ca^{2+}, and Cl^- which can be hazardous to the environment in large concentrations. In this subsection, we will study the fluid flows in porous media by considering the groundwater contamination modeled by the system (2.16) in Section 2. The relevant problems of groundwater contamination and the corresponding parameters can be referred to [33,25,10,34,17].

Considering the porous media $\overline{ABCD}$ in Fig. 7, the water enters this region from the left boundary $\overline{AD}$ and the polluting material is injected from a part boundary $\overline{EF}$ of top boundary with concentration $C = C^*$. Then the contaminant will be transported and diffused in the water flow. Neumann boundary conditions for mass transport are specified at two side boundaries $\overline{AD}$ and $\overline{BC}$. Neumann boundary conditions are also assumed across the bottom $\overline{AB}$ and along the top boundary $\overline{CD}$ for the flow and mass transport except at the source part $\overline{EF}$. The permeability are $k_x = 5 \times 10^{-11}$ m^2 and $k_z = 10^{-12}$ m^2. The diffusion coefficients of the polluting material are $D_{cx} = D_{cz} = 5 \times 10^{-3}$ m^2/*day*. The density of groundwater is $\rho = 1000$ kg/m^3 and the viscosity is $\mu = 0.001$ kg m^{-1} s^{-1}. The storage coefficient is $S_p = 10^{-5}$/m. The porosity is $\phi = 0.3$. The region is $\overline{AB} = 1000$ m long and $\overline{AD} = 20$ m deep. We also assume the polluting material is injected between $E = 100$ m point and $F = 125$ m point. The region is discretized by a regular spaced $\Delta x = 25$ m, $\Delta z = 0.5$ m network of 40 rows and 40 columns. The time step size is chosen to be $\Delta t = 10$ days. A flow from left to right is created across the region by fixing a water head of 20 m at the left side boundary and 15 m at the right side boundary. The initial condition of the water head is given as $H_0 = \frac{5}{10^6}(1000 - x)(1000 - x) + 15$. To investigate the contamination loading at $\overline{EF}$, we consider constant contamination loading rate at $\overline{EF}$.

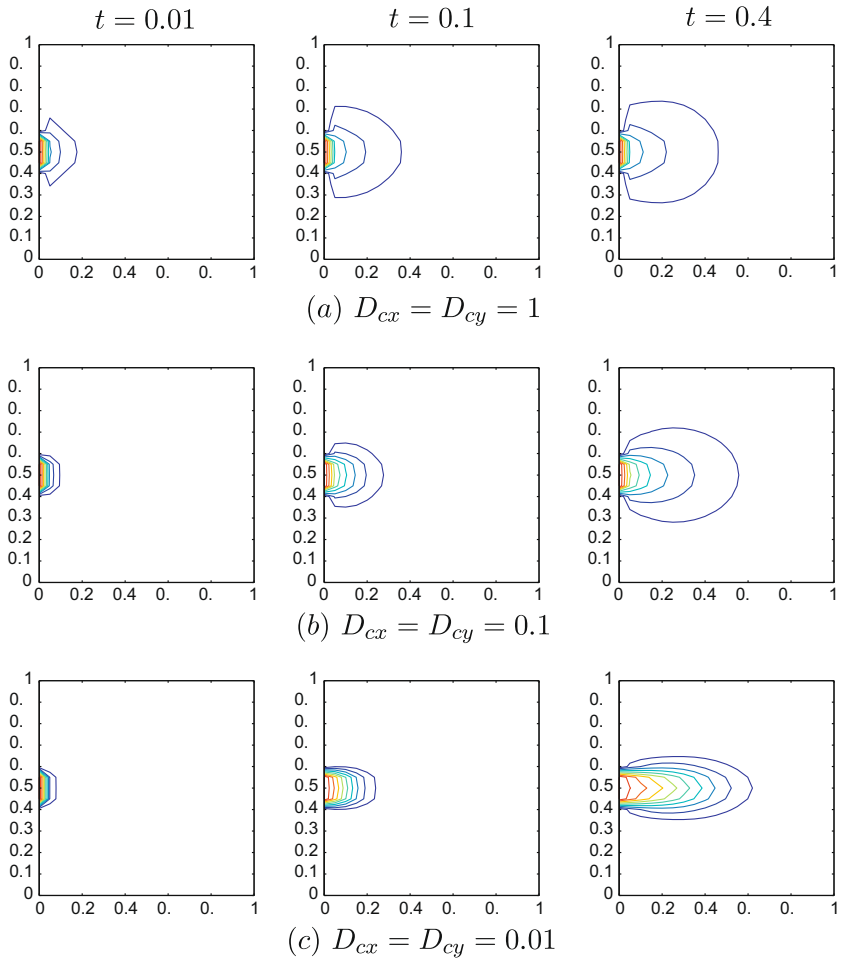

Fig. 5. The contour plots of concentration in homogenous flow with different diffusion coefficients in a velocity field $\mathbf{v} = (1, 0)^{\tau}$.

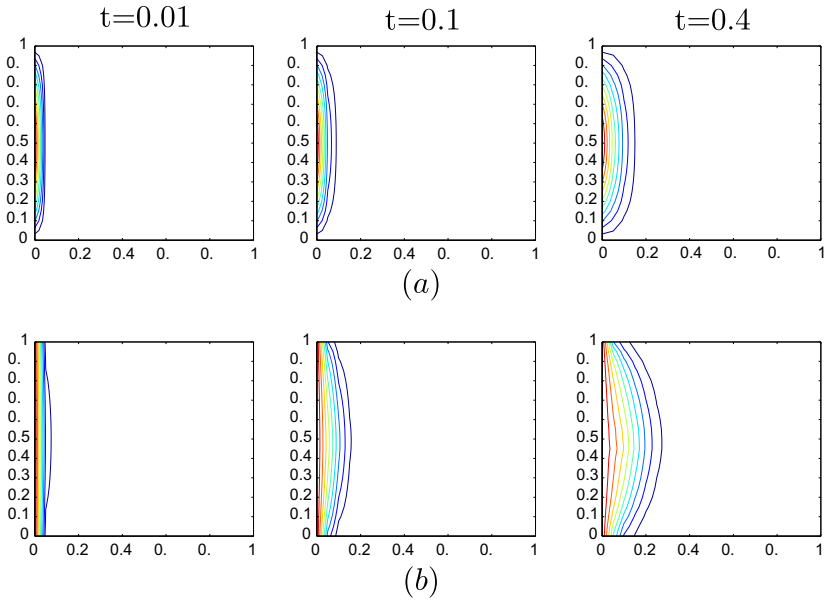

Fig. 6. The contour plots of the water head (a) and the concentration (b).

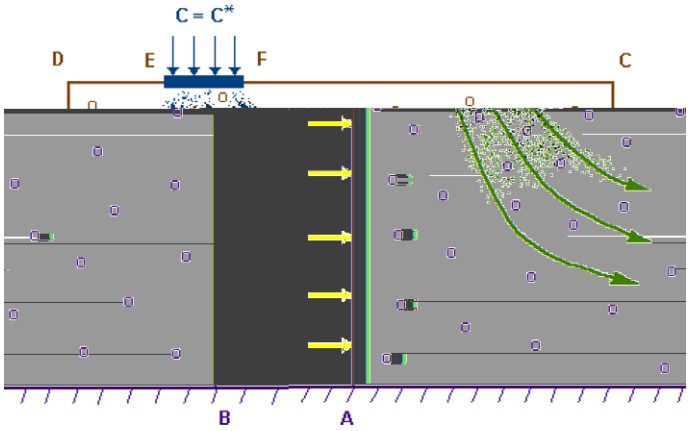

Fig. 7. Conceptual model of the pollution transport.

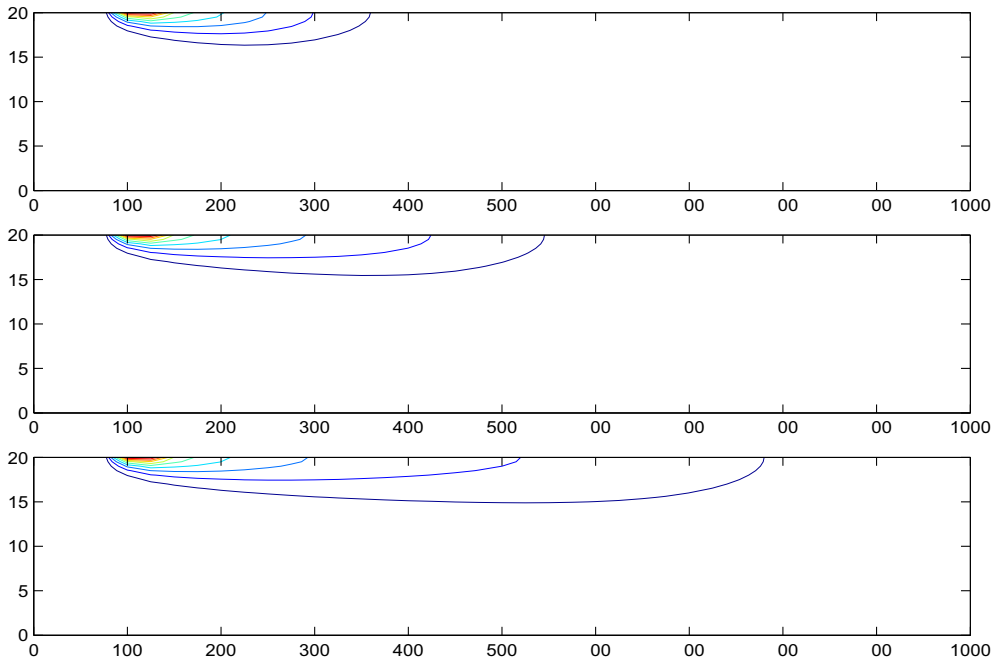

Fig. 8. The contour plots of concentration at t = 300 days, 600 days, and 1000 days.

4.2.1. Constant loading rate of contamination

We take the constant loading rate of contamination at $\overline{EF}$ with $c^* = 1\ \mathrm{kg/m^3}$. Fig. 8 presents the contour plots of the concentration of the contamination at 300 days, 600 days and 1000 days. With this constant contamination loading, it shows in the contour plots of concentration that the concentration transports along the flow. In the figures, we also see that the concentration decreases as the contamination front is propagated away from the original loading location $\overline{EF}$.

4.3. Concentration dependent density and layered media

In this subsection, we carry out numerical simulations to compressible fluid flows with concentration dependent density and to compressible fluid flows in layered media, which are often encountered in many field applications [33,25,10,34,17].

4.3.1. Concentration dependent density

The approximation of the concentration dependent density of mixtures are complicated because there is no exact equation to relate the density to the concentrations. From the Hugakorn's linearization (2.15), the density of an aqueous mixture

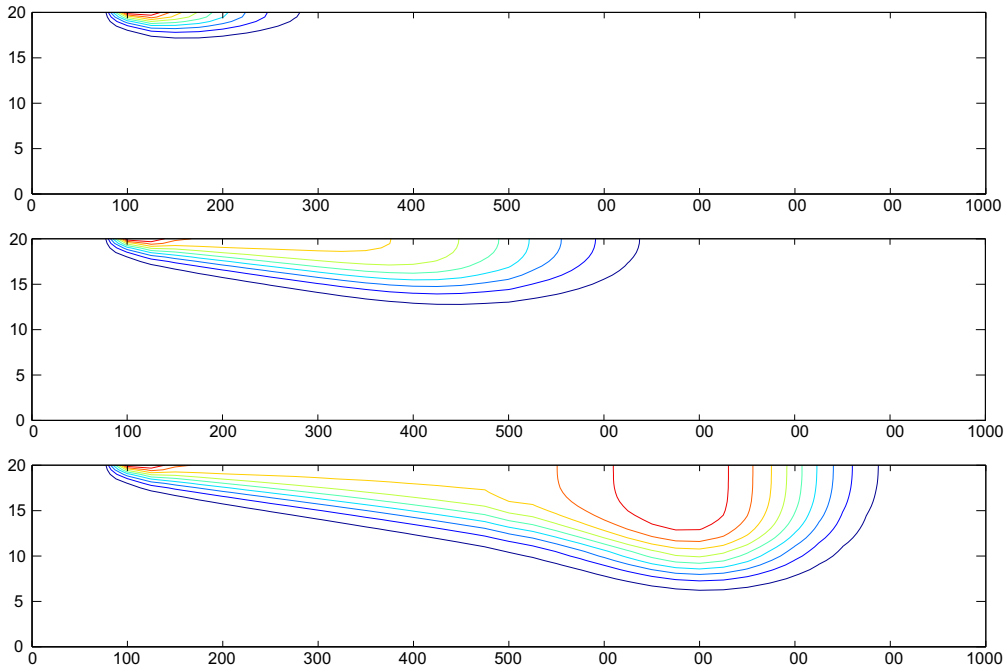

Fig. 9. The contour plots of fluid flow with concentration dependent density at t = 100 days, 500 days and 1000 days.

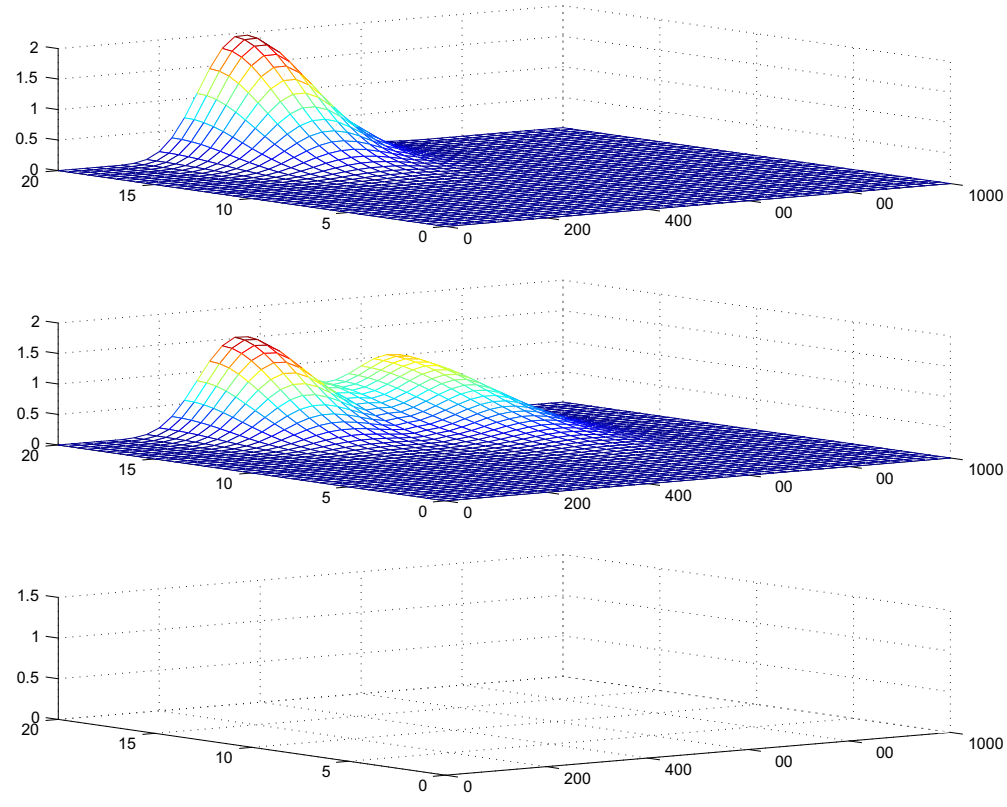

ρ for a dilute solution can be described as a linear function of concentration, i.e., a first order approximation of density has the form $\rho = \rho_0(1 + \eta c)$, where η is a small number $0 < \eta \leqslant 1$ and ρ_0 is the reference density. We choose $\eta = 0.005$ in this test and other parameters same as those in the previous subsection. The contamination is constantly injected into the domain through $\overline{EF}$ with $c^* = 2\text{kg/m}^3$. By the S-DDM method, we simulate the procedure of the contamination transport. The contour plots of the contamination at the time t = 100 days, 500 days and 1000 days are presented in Fig. 9. Comparing Fig. 8 with Fig. 9, we can see that the contaminant front moves faster along the vertical direction in Fig. 9, because the velocity gets bigger when the density is concentration dependent.

4.3.2. Intermittent injecting rate of contamination

The contamination injection can appear to be intermittent, e.g. the source loading from the Babylon Landfill. In this test, we consider the problems with intermittent injecting rate of contamination. Take $\eta = 0.005$ and the initial value of water head $H_0 = \frac{5}{10^6}(1000 - x)(1000 - x) + 15$. The contaminate loading rate at the top boundary $\overline{EF}$ is assumed to occur only for the first 100 days with the concentration 18 kg/m^3, the fifth 100 days with the concentration 15 kg/m^3 and the eighth 100 days with the concentration 4 kg/m^3. Fig. 10 presents the concentration distribution of contaminant at different time t = 300 days, 700 days and 900 days. From the first graph in Fig. 10, after the first 100 days, the first contaminate region is beginning to form at the top boundary $\overline{EF}$. The second graph of Fig. 10, which encompasses two periods of the concentration of the contamination, shows how after 700 days two contaminate regions have been formed. In the last graph, after 900 days, three contaminating cells have been formed. It also shows that the contamination transport along the flow is accompanied by dispersion, which reduces the concentration in these cells.

4.3.3. Fluid flows in layered media

In many real problems, the media is not homogeneous. In this test, we consider layered media. We simulate fluid flows in a layered medium in which one highly permeable zone is located at the bottom. In the whole region the permeability in vertical direction $k_z = 1 \times 10^{-12}$ m^2, while the permeability in horizontal direction is $k_{x,1} = 2 \times 10^{-11}$ m^2 in the upper region, $x \in [0, 1000]$, $z \geqslant 10$ and $k_{z,2} = 8 \times 10^{-11}$ m^2 in the bottom region, $x \in [0, 1000], z \leqslant 10$. Let $\eta = 0.004$. The contour plots of the concentration of the contamination at t = 1000 days, t = 1500 days and t = 1800 days are presented in Fig. 11. From this figure, we can see that the concentration front moves faster in the horizontal direction than in the vertical direction, because the porous media has larger permeability in horizontal direction, and thus, the velocity in horizontal direction is bigger than that in vertical direction. Moreover, once the flow invades into the bottom region, the concentration front moves much faster in the horizontal direction in bottom region than in upper region, and exhibits the behavior of a layered flow.

We also consider another case for layered media where the permeability are $k_{x,1} = 2 \times 10^{-11}$ m^2 and $k_{z,1} = 1 \times 10^{-12}$ m^2 along horizontal and vertical directions, respectively, in the upper region, and $k_{x,2} = 8 \times 10^{-11}$ m^2 and $k_{z,2} = 4 \times 10^{-12}$ m^2 along horizontal and vertical directions, respectively, in the bottom region. The contour plots of the concentration of the

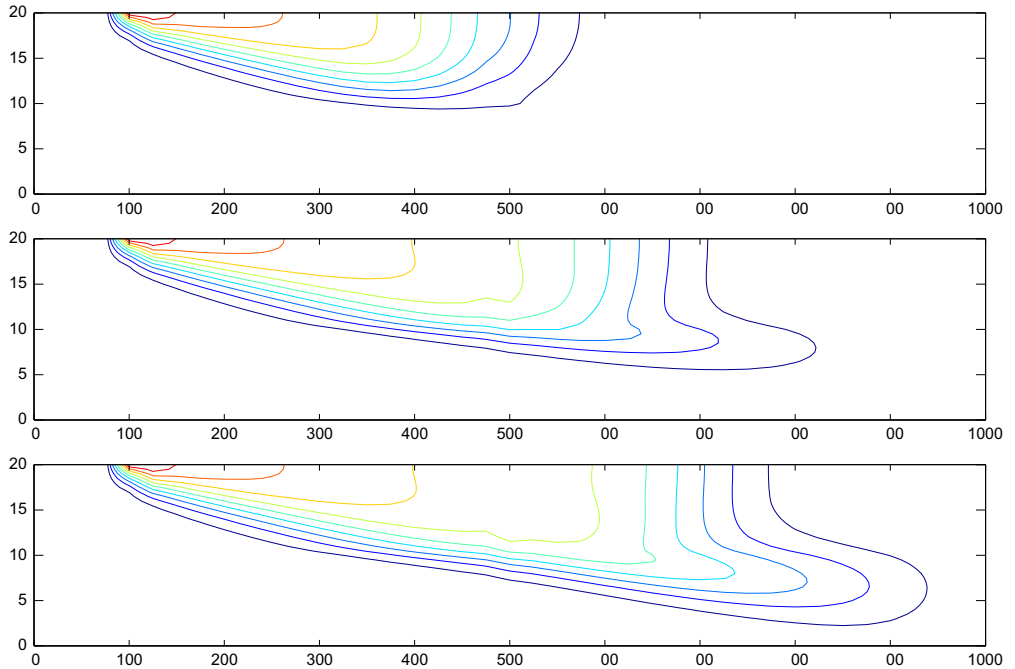

Fig. 11. The contour plots of fluid flows in layered media at t = 1000 days, 1500 days and 1800 days.

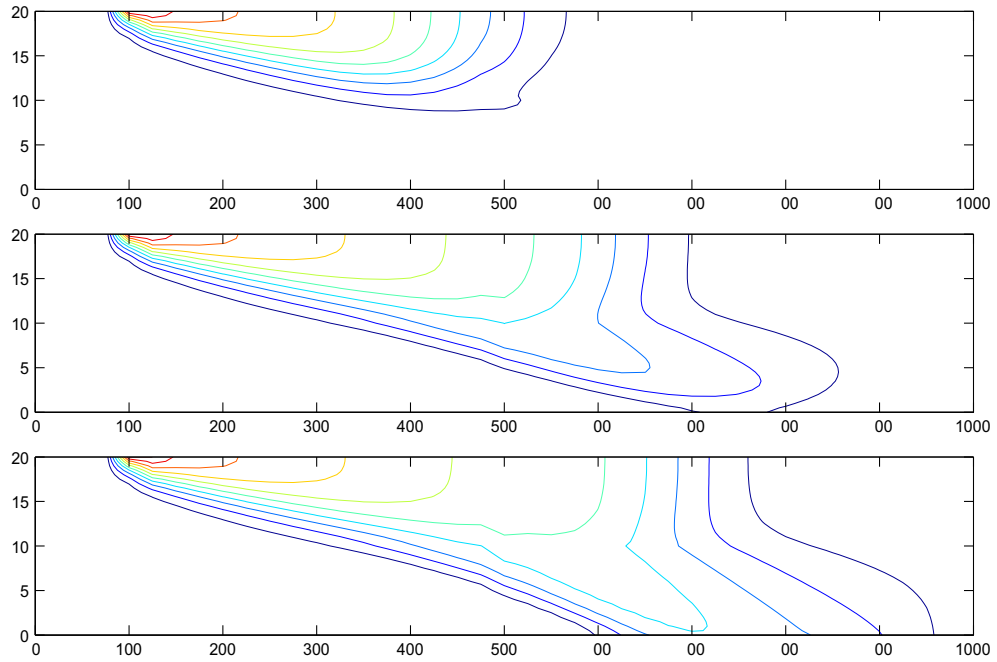

Fig. 12. The contour plots of fluid flows in layered media at t = 1000 days, 1500 days and 1800 days.

contamination at t = 1000 days, t = 1500 days and t = 1800 days are presented in Fig. 12. Similarly, we can see that the concentration front moves faster in the horizontal direction than in the vertical direction, and also after the flow invading into the bottom region, the concentration front moves much faster in both horizontal and vertical directions in bottom region than in upper region.

5. Conclusions

In this paper,we developed a new efficient S-DDM iterative approach for compressible contamination fluid flows in porous media. The S-DDM iterative approach divides the large domain into multiple block sub-domains. In each time interval, firstly the S-DDM scheme is applied to solve the water head equation, in which we use a local multilevel scheme for computing water head values on the interfaces of the sub-domains and use the splitting implicit scheme to solve the interior values of water head in sub-domains; then S-DDM scheme combining upstream technique is proposed to solve the concentration equation. The S-DDM iterative approach reduces computational complexities, large memory requirements and long computation durations.

In numerical experiments, we firstly carried out numerical simulations of homogenous flows by using the developed S-DDM approach, showing the efficient approximation meanwhile ensuring the accuracy. In the second experiment, we presented numerical results for groundwater contaminations with the continuous contamination loading. The numerical simulations appear to reproduce qualitatively the major characteristics of the propagation of the contamination in porous media flows. In the third experiment, we simulated fluid flows with concentration dependent density and fluid flows in the layered porous media. Numerical results showed the efficient performance of the S-DDM iterative approach to simulate fluid flows in porous media.

The developed S-DDM iterative approach provides feasibly and powerfully approximating to contamination fluid flows in porous media and can be extended to multi-dimensional and multi-components fluid flows in porous media as well as to multi-phase fluid flows in porous media which leave as our near future work.

Acknowledgments

This research was partially supported by the Natural Sciences and Engineering Research Council of Canada (NSERC) and by Mathematics for Information Technology and Complex Systems (MITACS). We would thank the referees and the editor for their valuable suggestions which have helped to improve the paper greatly.

References

[1] K. Aziz, A. Settari, Petroleum Reservoir Simulation, Applied Science Publisher LTD, London, 1979.
[2] V. Batu, Applied Flow and Solute Transport Modeling in Aquifers, CRC Press, 2005.

[3] J. Bear, Hydraulics of Groundwater, McGraw-Hill, New York, 1978.
[4] W. Chen, X. Li, D. Liang, Energy-conserved splitting FDTD methods for Maxwell's equations, Numer. Math. 108 (3) (2008) 445–485.
[5] W. Chen, X. Li, D. Liang, Symmetric energy-conserved splitting FDTD scheme for the Maxwell's equations, Commun. Comput. Phys. 6 (2009) 804–825.
[6] Z. Chen, G. Huan, Y. Ma, Computational Methods for Multiphase Flows in Porous Media, Computational Science and Engineering Series, vol. 2, SIAM, Philadelphia, 2006.
[7] C. Clavero, J.C. Jorge, F. Lisbona, G.I. Shishkin, A fractional step method on a special mesh for the resolution of multidimensional evolutionary convection–diffusion problems, Appl. Numer. Math. 27 (1998) 211–231.
[8] W. Dai, N. Raja, A new ADI scheme for solving three-dimensional parabolic equations with first-order derivatives and variable coefficients, J. Comput. Anal. Appl. 122 (1995) 223–250.
[9] C.N. Dawson, Q. Du, T.F. Dupont, A finite difference domain decomposition algorithm for numerical solution of the heat equation, Math. Comp. 57 (1991) 63–71.
[10] H.-J. Diersch, O. Kolditz, Variable-density flow and transport in porous media: approaches and challenges, Adv. Water Resour. 25 (2002) 899–944.
[11] J. Douglas Jr., D. Peaceman, Numerical solution of two dimensional heat flow problem, Am. Inst. Chem. Eng. J. 1 (1955) 505–512.
[12] J. Douglas Jr., S. Kim, Improved accuracy for locally one-dimensional methods for parabolic equations, Math. Model Meth. Appl. Sci. 11 (2001) 1563–1579.
[13] Q. Du, M. Mu, Z.N. Wu, Efficient parallel algorithms for parabolic problems, SIAM J. Numer. Anal. 39 (2001) 1469–1487.
[14] R.E. Ewing, The Mathematics of Reservoir Simulation, Frontiers in Applied mathematics, vol. 1, SIAM, Philadelphia, 1983.
[15] M. Feistauer, J. Felcman, I. Straskraba, Mathematical and Computational Methods for Compressible Flow, Oxford University Press, 2003.
[16] P.A. Forsyth, A control volume finite element approach to NAPL groundwater contamination, SIAM J. Sci. Stat. Comp. 12 (1991) 1029–1057.
[17] P. Frolkovic, H. De Schepper, Numerical modelling of convection dominated transport coupled with density driven flow in porous media, Adv. Water Resourc. 24 (1) (2001) 63–72.
[18] S. Gaiffe, R. Glowinski, R. Lemonnier, Domain decomposition and splitting methods for parabolic problems via a mixed formulation, in: The 12th International Conference on Domain Decomposition, Chiba, Japan, 1999.
[19] L.P. Gao, B. Zhang, D. Liang, Splitting finite difference methods on staggeres grids for three-dimensional time-dependent Maxwell equations, Commun. Comput. Phys. 4 (2008) 405–432.
[20] K.H. Karlsen, K.-A. Lie, An unconditionally stable splitting scheme for a class of nonlinear parabolic equations, IMA J. Numer. Anal. 19 (1999) 1–28.
[21] Y.A. Kuznetsov, New algorithm for approximate realization of implicit difference schemes, Soviet J. Numer. Anal. Math. Model. 3 (1988) 99–114.
[22] D. Liang, W. Zhao, An optimal weighted upwinding covolume method on non-standard grids for convection–diffusion problems in 2D, Int. J. Numer. Meth. Eng. 67 (4) (2006) 553–577.
[23] P.L. Lions, On the Schwarz alternating method I, in: R. Glowinskin, G.H. Golub, G.A. Meurant, J. Periaux (Eds.), Proceedings of the First International Symposium on Domain Decomposition Methods for Partial Differential Equations, Paris, 1987, SIAM, Philadelphia, USA, 1988, pp. 1–42.
[24] P.L. Lions, On the Schwarz alternating method II, in: T. Chan, R. Glowinskin, J. Periaux, O. Wildlund (Eds.), Proceedings of the Second International Symposium on Domain Decomposition Methods for Partial Differential Equations, Los Angeles, 1988, SIAM, Philadelphia, USA, 1989, pp. 47–70.
[25] A. Mazzia, M. Putti, Three-dimensional mixed finite element-finite volume approach for the solution of density-dependent flow in porous media, J. Comp. Appl. Math. 185 (2006) 347–359.
[26] K.A. Narayan, C. Schleeberger, K.L. Bristow, Modelling seawater intrusion in the Burdekin Delta Irrigation Area, North Queensland, Australia, Agric. Water Manage. 89 (3) (2007) 217–228.
[27] Y.J. Park, E.A. Sudicky, S. Panday, J.F. Sykes, V. Guvanasen, Application of implicit sub-time stepping to simulate flow and transport in fractured porous media, Adv. Water Resourc. 31 (2008) 995–1003.
[28] L. Portero, J.C. Jorge, A generalization of Peaceman–Rachford fractional step method, J. Comp. Appl. Math. 189 (1) (2006) 676–688.
[29] B.F. Smith, P.E. Bjost, W.D. Gropp, Domain Decomposition Methods for Partial Differential Equations, Cambridge University Press, 1996.
[30] G. Strang, On the construction and comparison of difference schemes, SIAM J. Numer. Anal. 5 (1968) 506–517.
[31] N. Yanenko, The Method of Fractional Steps, Springer-Verlag, Berlin, Heidelberg, New York, 1971.
[32] Y. Yuan, D. Liang, H. Rui, Characteristics-finite element methods for seawater intrusion numerical simulation and theoretical analysis, Acta Math. Appl. Sinica 14 (1998) 12–23.
[33] H. Zhang, F.W. Schwartz, Multispecies contaminant plumes in variable density flow systems, Water Resourc. Res. 31 (4) (1995) 837–847.
[34] S. Zimmermann, P. Bauer, R. Held, W. Kinzelbach, J.H. Walther, Salt transport on islands in the Okavango Delta: numerical investigations, Adv. Water Resourc. 29 (2006) 11–29.